

AI-Based Image Formation

Marc Kachelrieß

German Cancer Research Center (DKFZ)

Heidelberg, Germany

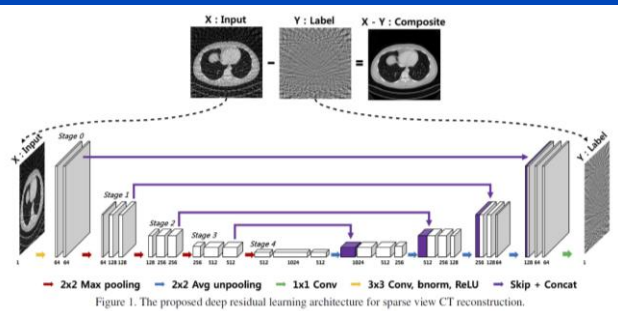
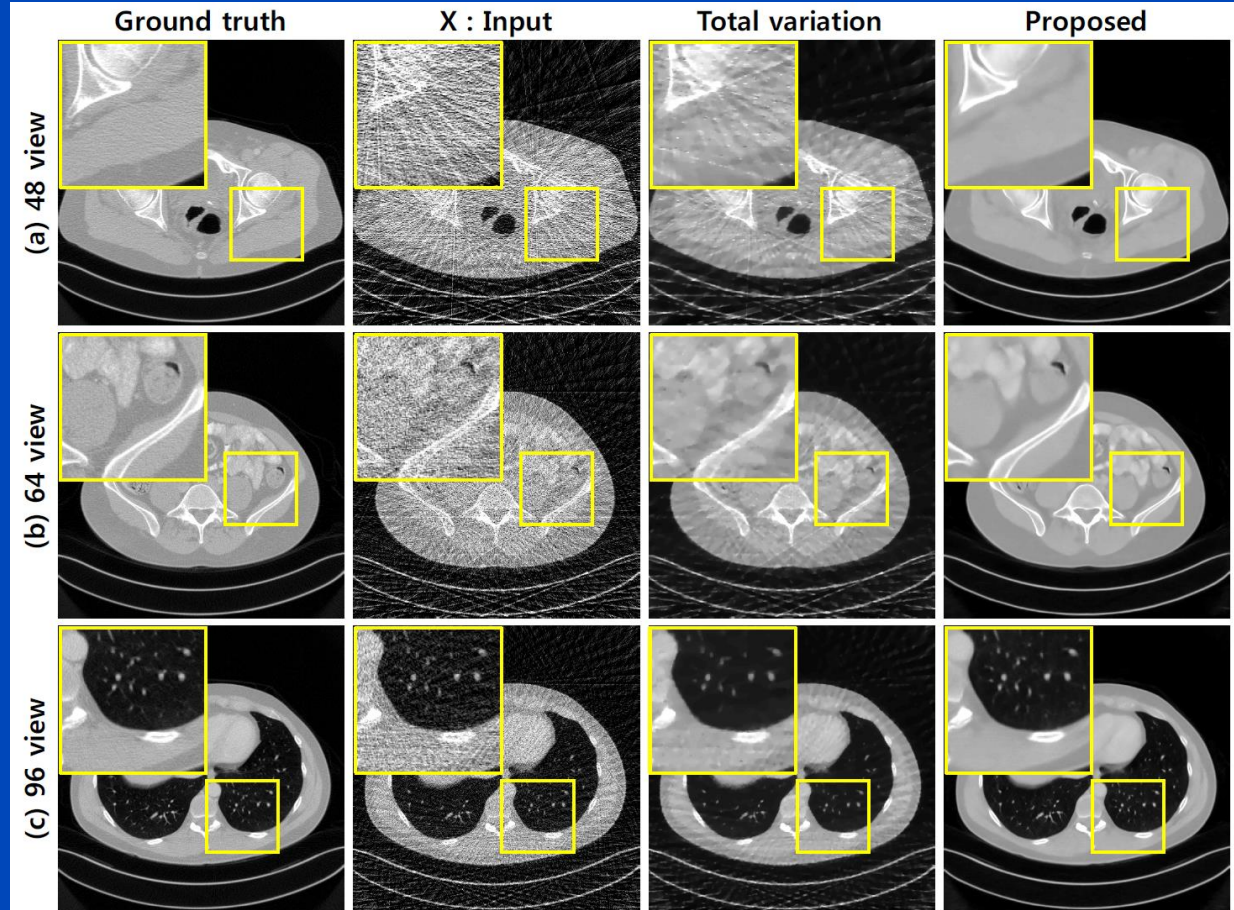
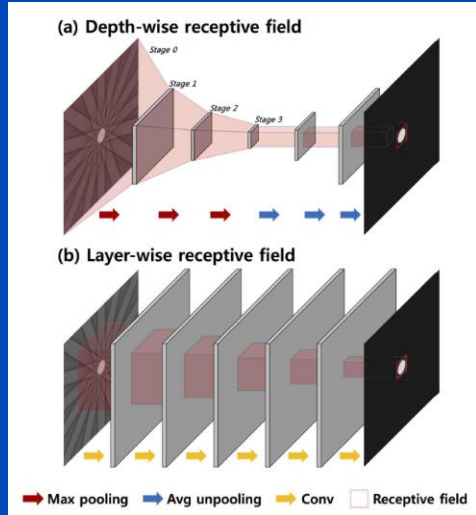
www.dkfz.de/ct



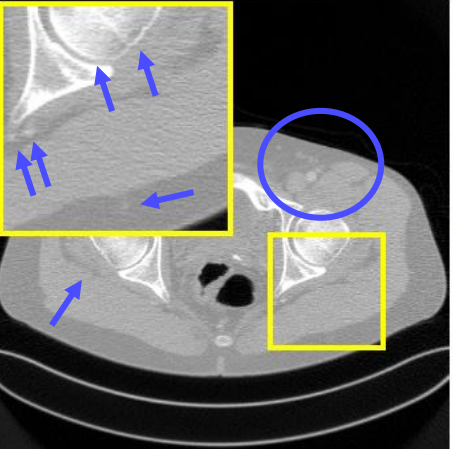
DEUTSCHES
KREBSFORSCHUNGZENTRUM
IN DER HELMHOLTZ-GEMEINSCHAFT

Dose Reduction

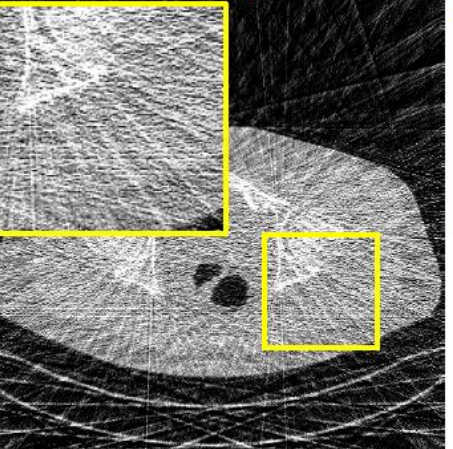
Sparse View Restoration Example



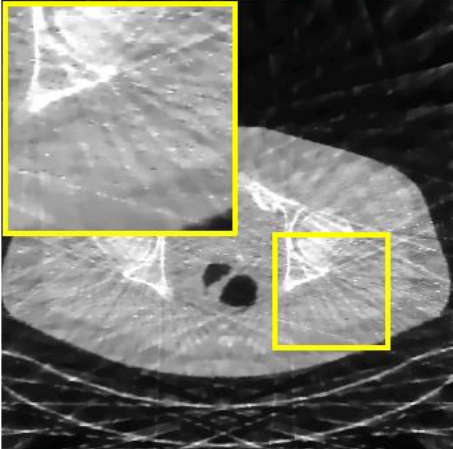
Ground truth



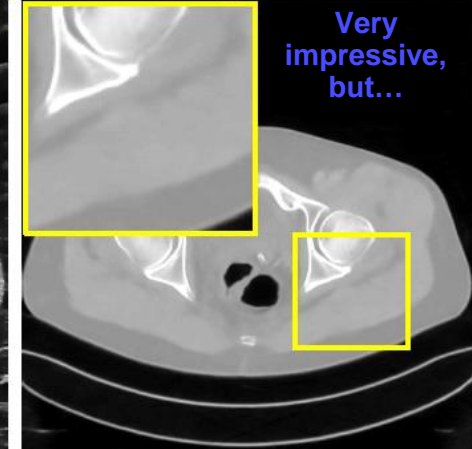
X : Input



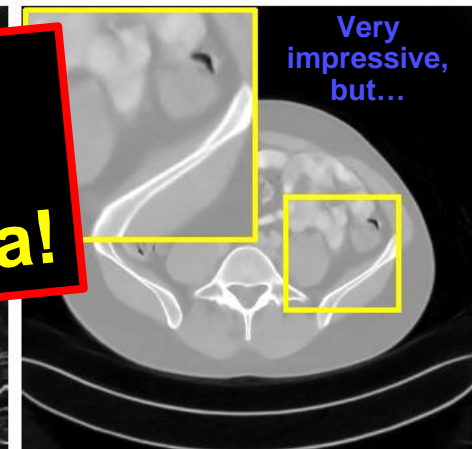
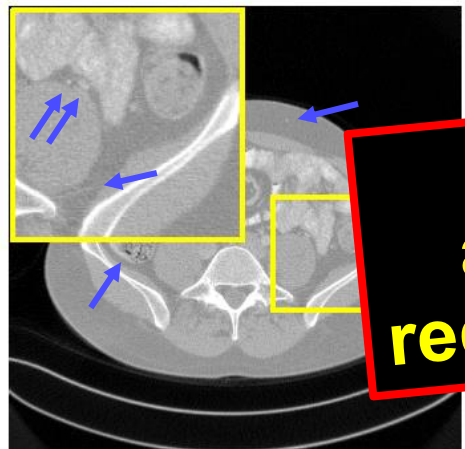
Total variation



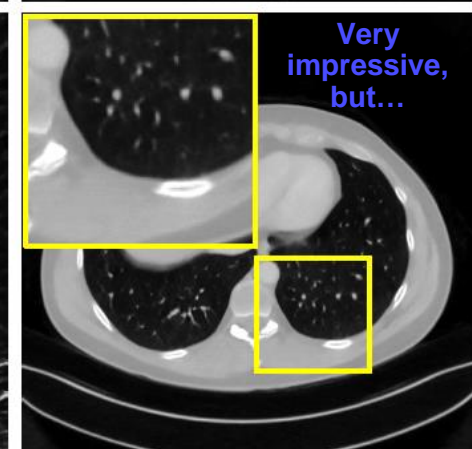
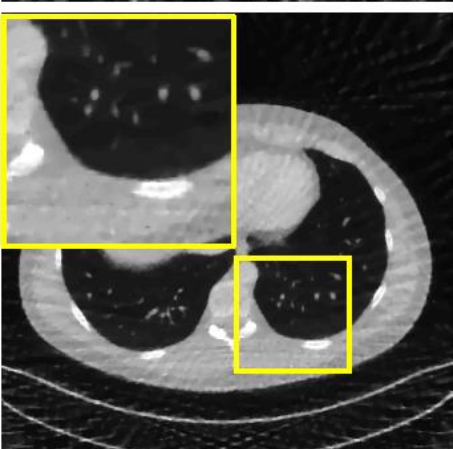
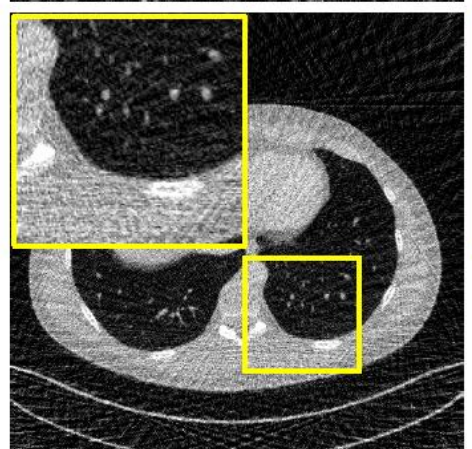
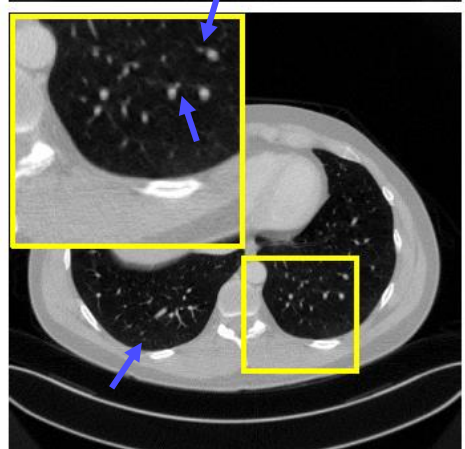
Proposed



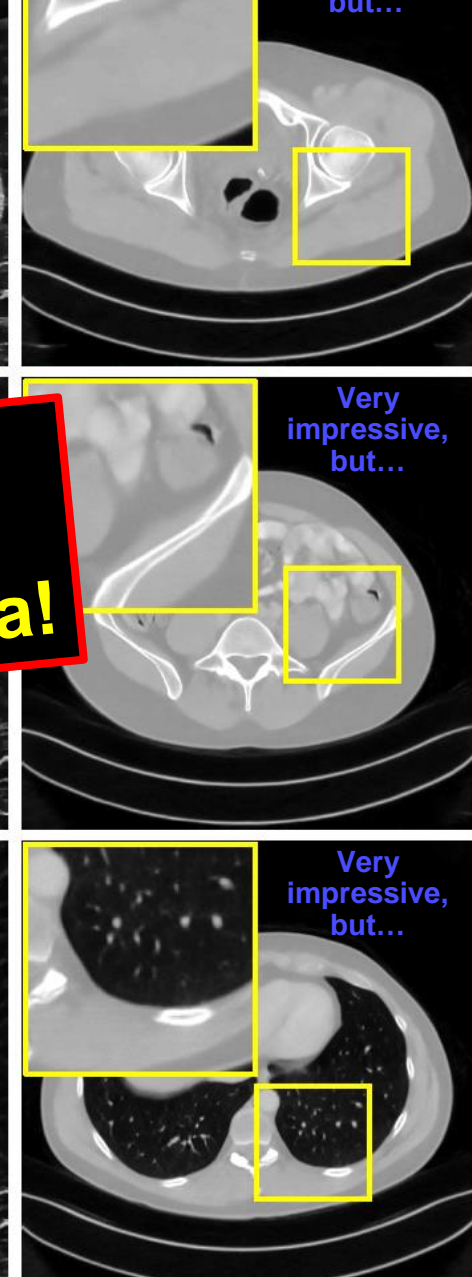
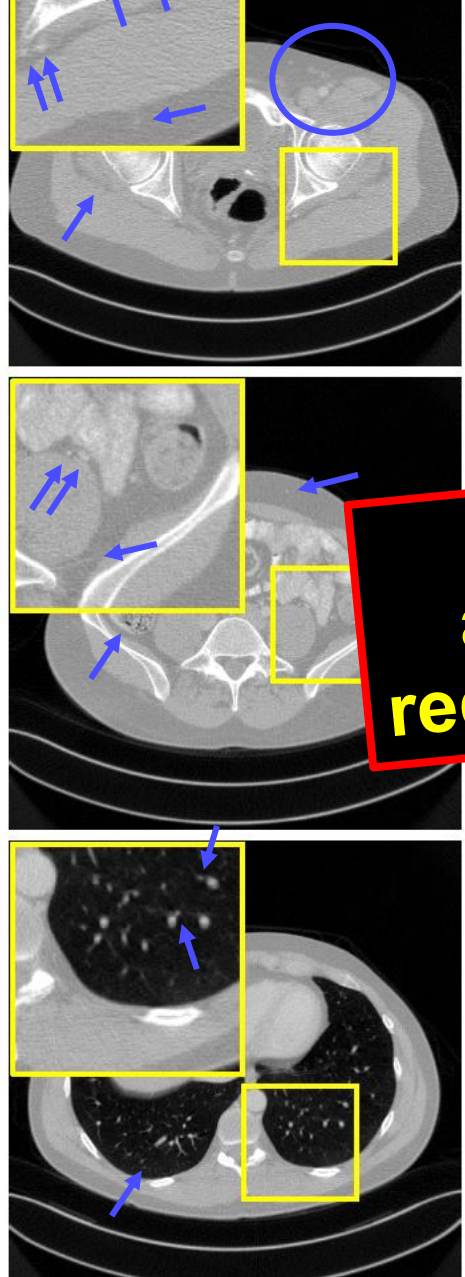
(a) 48 view



(b) 64 view

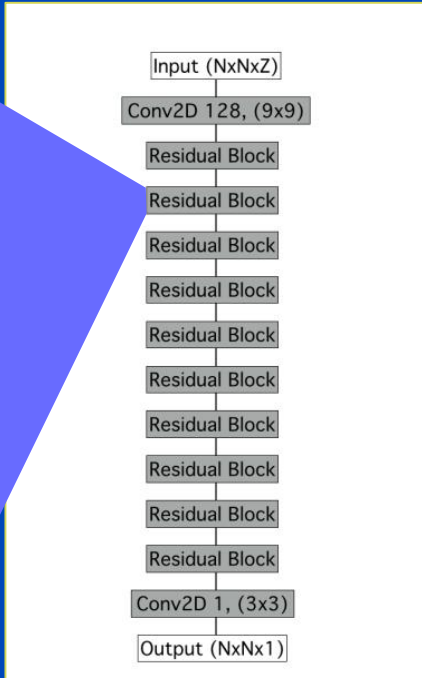
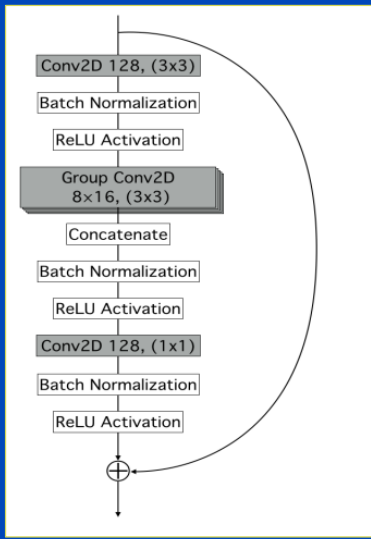


(c) 96 view

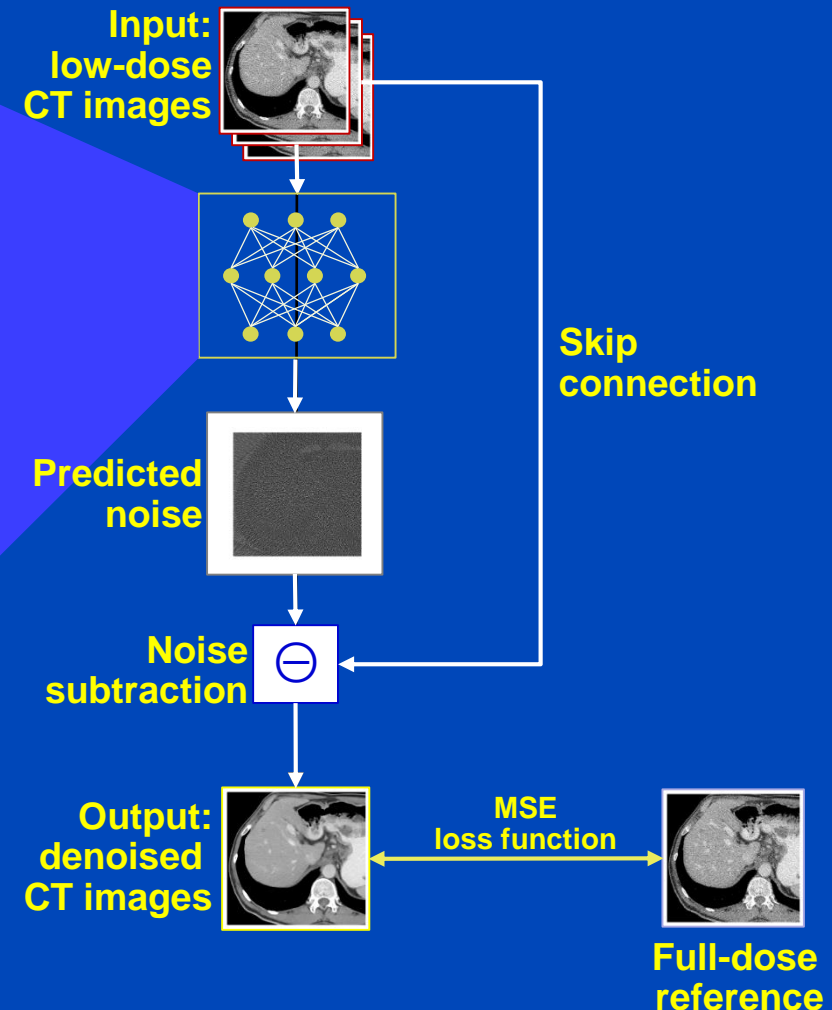


Proposing sparse
acquisitions just for dose
reduction is NOT a good idea!

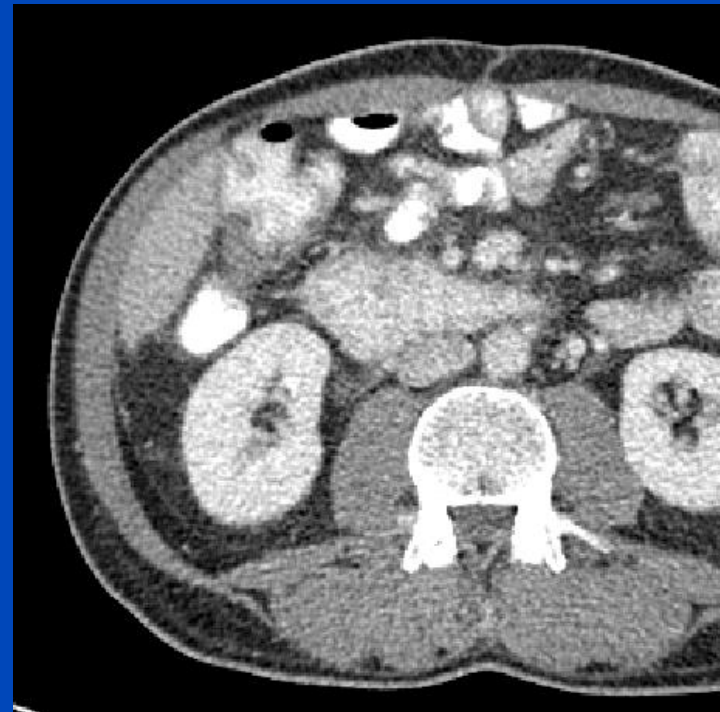
Noise Removal



- Architecture based on state-of-the-art networks for image classification (ResNet).
- 32 conv layers with skip connections
- About 2 million tunable parameters in total
- Input is arbitrarily-size stack of images, with a fixed number of adjacent slices in the channel/feature dimension.



Noise Removal



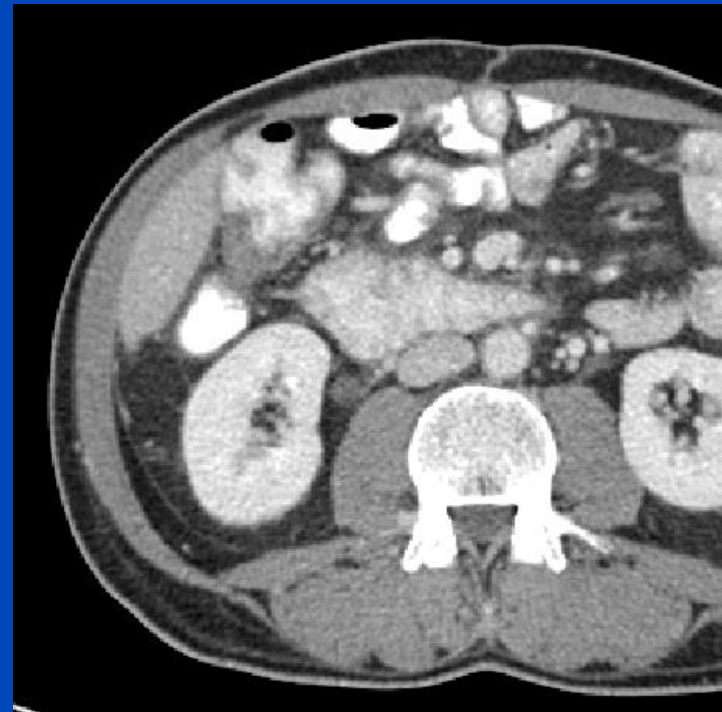
Low dose images (1/4 of full dose)

Noise Removal



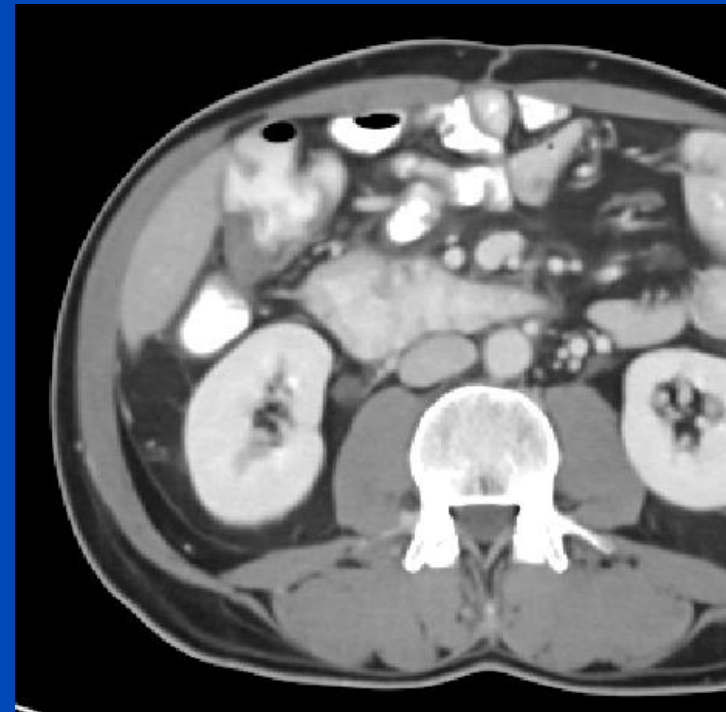
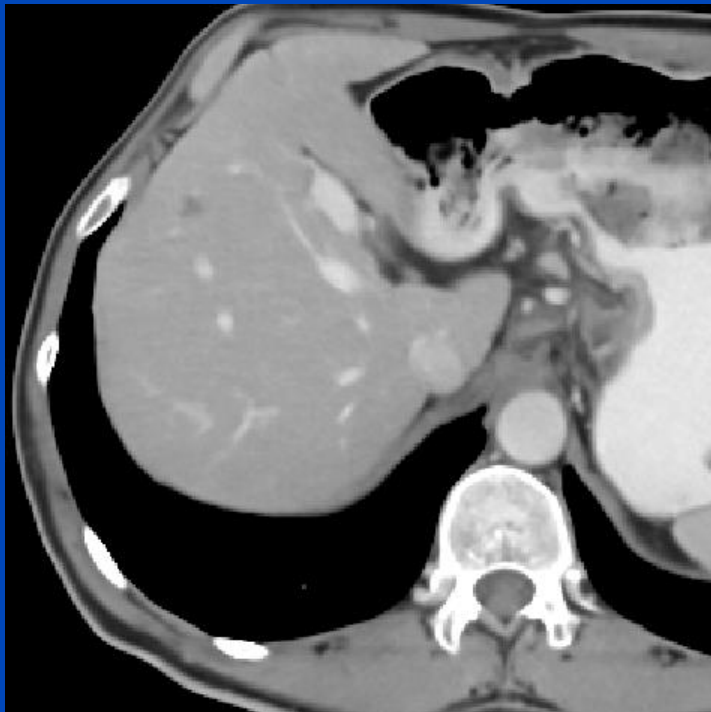
Denoised low dose

Noise Removal



Full dose

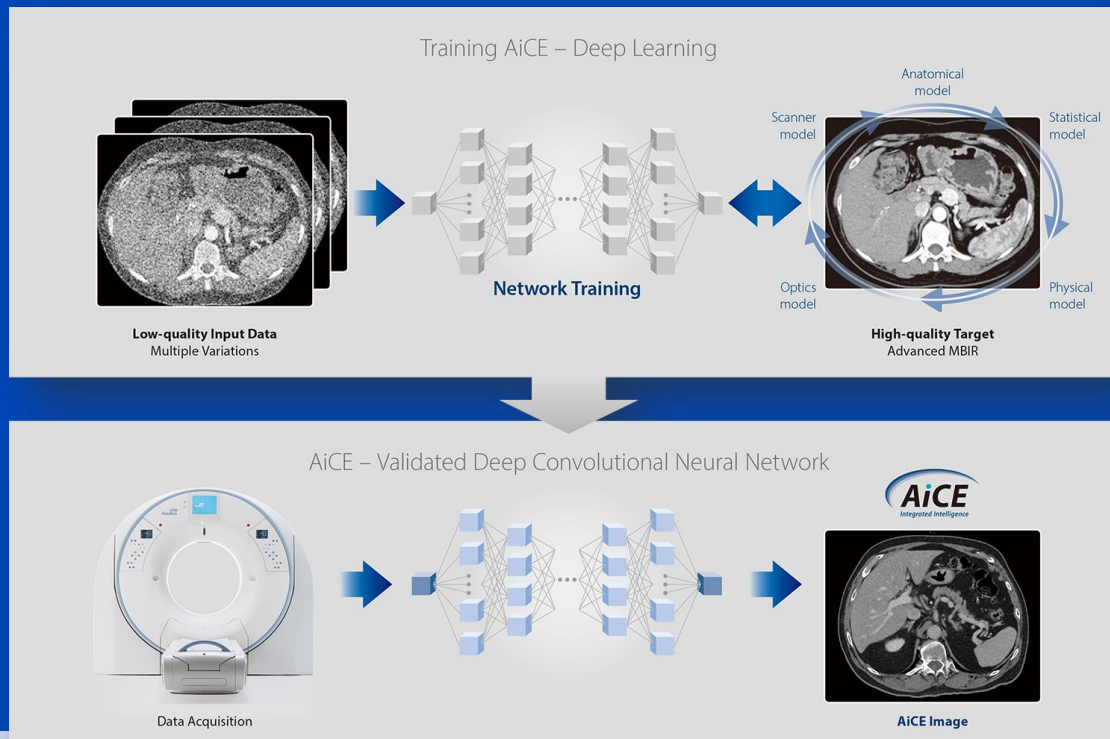
Noise Removal



Denoised full dose

Canon's AiCE

- Advanced intelligent Clear-IQ Engine (AiCE)
- Trained to restore low-dose CT data to match the properties of FIRST, the model-based IR of Canon.
- FIRST is applied to high-dose CT images to obtain a high fidelity training target

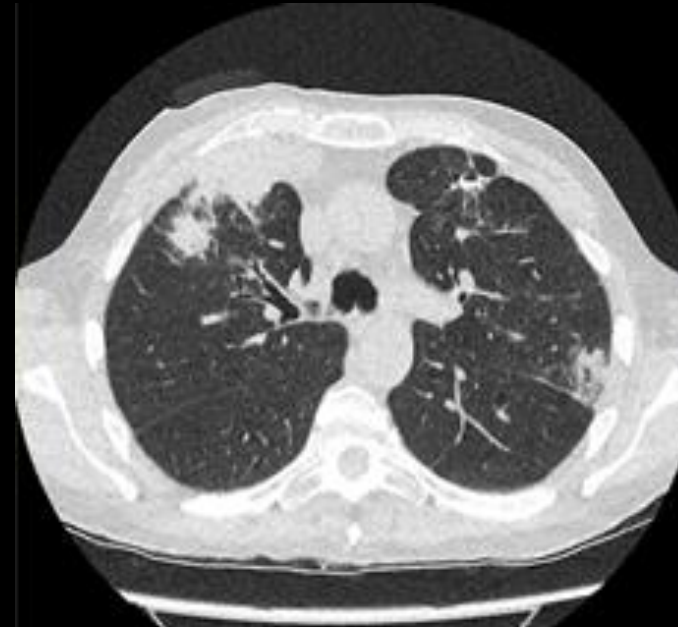


Information taken from https://global.medical.canon/products/computed-tomography/aice_dlr

$U = 100 \text{ kV}$
 $\text{CTDI} = 0.6 \text{ mGy}$
 $\text{DLP} = 24.7 \text{ mGy}\cdot\text{cm}$
 $D_{\text{eff}} = 0.35 \text{ mSv}$



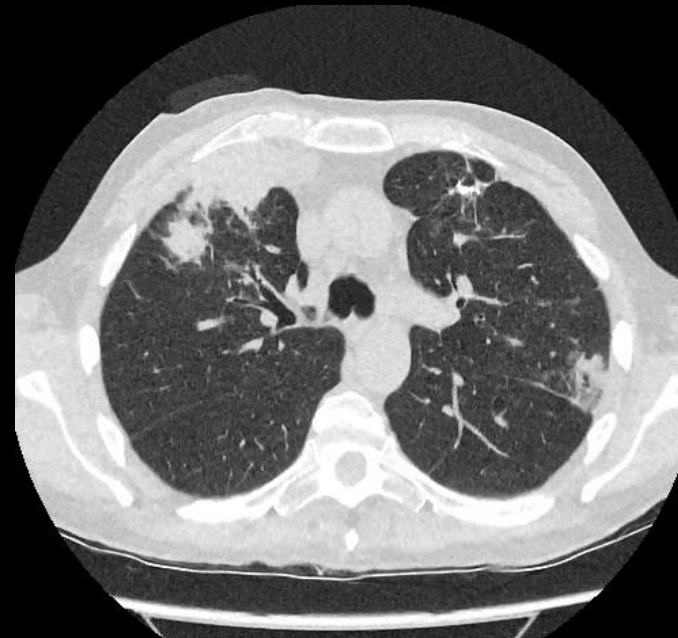
FBP FC52 (analytical recon)



AIDR3De FC52 (image-based iterative)



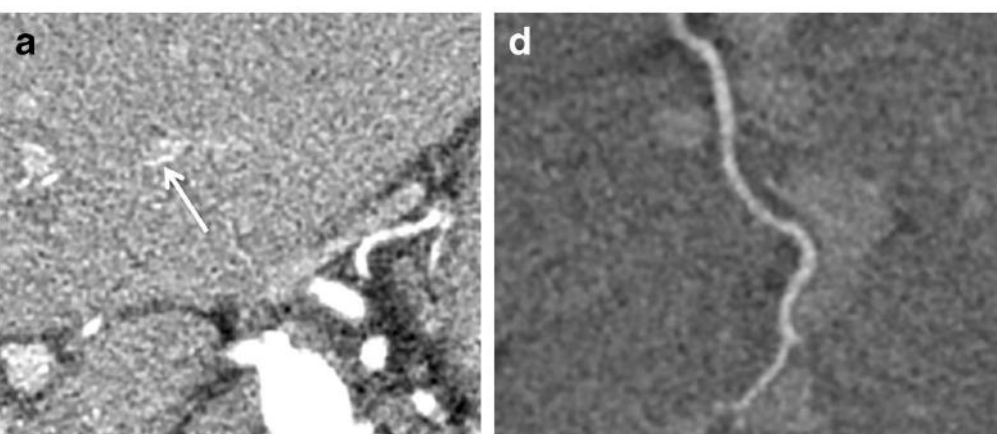
FIRST Lung (full iterative)



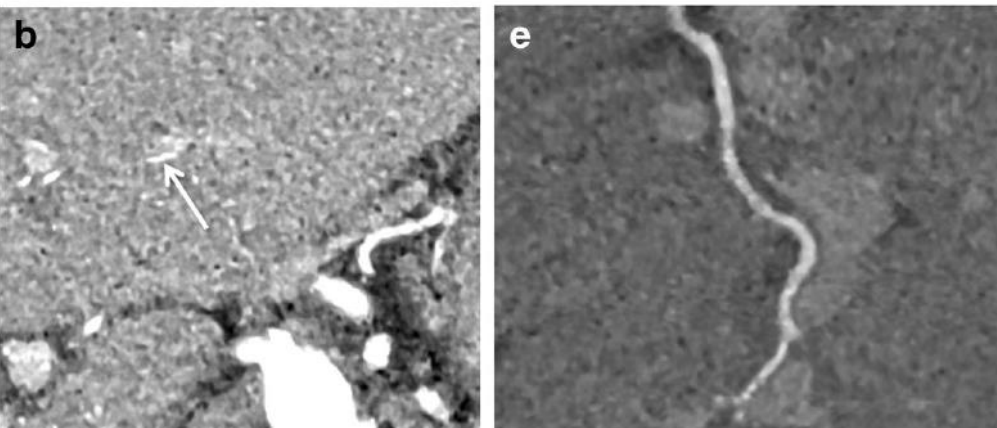
AiCE Lung (deep learning)

Courtesy of
Radboudumc,
the Netherlands

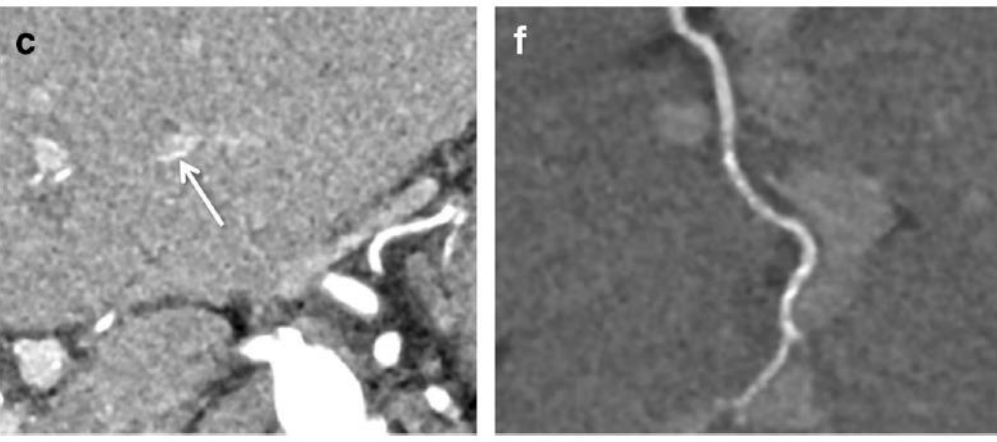
AIDR 3D



First



AiCE



GE's True Fidelity

- Based on a deep CNN
- Trained to restore low-dose CT data to match the properties of Veo, the model-based IR of GE.
- No information can be obtained in how the training is conducted for the product implementation.

SS.IV] 20 Dec 2018

2.5D DEEP LEARNING FOR CT IMAGE RECONSTRUCTION USING A MULTI-GPU IMPLEMENTATION

Amirkoushyar Ziabari^{}, Dong Hye Ye ^{* †}, Somesh Srivastava[‡], Ken D. Sauer [⊕]
Jean-Baptiste Thibault [‡], Charles A. Bouman^{*}*

^{*} Electrical and Computer Engineering at Purdue University
[†] Electrical and Computer Engineering at Marquette University
[‡] GE Healthcare
[⊕] Electrical Engineering at University of Notre Dame

ABSTRACT

While Model Based Iterative Reconstruction (MBIR) of CT scans has been shown to have better image quality than Filtered Back Projection (FBP), its use has been limited by its high computational cost. More recently, deep convolutional neural networks (CNN) have shown great promise in both denoising and reconstruction applications. In this research, we propose a fast reconstruction algorithm, which we call Deep

streaking artifacts caused by sparse projection views in CT images [8]. More recently, Ye, et al. [9] developed method for incorporating CNN denoisers into MBIR reconstruction as advanced prior models using the Plug-and-Play framework [10,11].

In this paper, we propose a fast reconstruction algorithm, which we call Deep Learning MBIR (DL-MBIR), for approximately achieving the improved quality of MBIR using a deep residual neural network. The DL-MBIR method is trained to



FBP

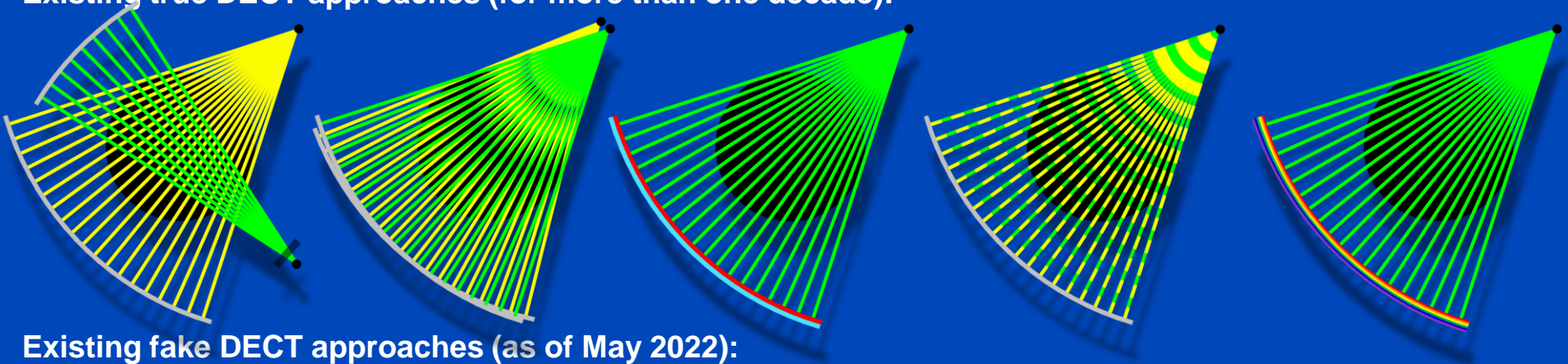
ASIR V 50%

True Fidelity

Courtesy of GE Healthcare

True and Fake DECT

Existing true DECT approaches (for more than one decade):



Existing fake DECT approaches (as of May 2022):

- [1] J. Ma, Y. Liao, Y. Wang, S. Li, J. He, D. Zeng, Z. Bian, “**Pseudo dual energy CT imaging using deep learning-based framework: basic material estimation**”, *SPIE Medical Imaging 2018*.
- [2] W. Zhao, T. Lv, P. Gao, L. Shen, X. Dai, K. Cheng, M. Jia, Y. Chen, L. Xing, “A deep learning approach for dual-energy CT imaging **using a single-energy CT data**”, *Fully3D 2019*.
- [3] D. Lee, H. Kim, B. Choi, H. J. Kim, “Development of a deep neural network for generating synthetic dual-energy chest x-ray images **with single x-ray exposure**”, *PMB 64(11)*, 2019.
- [4] L. Yao, S. Li, D. Li, M. Zhu, Q. Gao, S. Zhang, Z. Bian, J. Huang, D. Zeng, J. Ma, “Leveraging deep generative model for direct energy-resolving CT imaging **via existing energy-integrating CT images**”, *SPIE Medical Imaging 2020*.
- [5] D. P. Clark, F. R. Schwartz, D. Marin, J. C. Ramirez-Giraldo, C. T. Badea, “Deep learning based **spectral extrapolation** for dual-source, dual-energy x-ray CT”, *Med. Phys. 47 (9): 4150–4163*, 2020.
- [6] C. K. Liu, C. C. Liu, C. H. Yang, H. M. Huang, “Generation of brain dual-energy CT **from single-energy CT** using deep learning”, *Journal of Digital Imaging 34(1):149–161*, 2021.
- [7] T. Lyu, W. Zhao, Y. Zhu, Z. Wu, Y. Zhang, Y. Chen, L. Luo, S. Li, L. Xing, “Estimating dual-energy CT imaging **from single-energy CT** data with material decomposition convolutional neural network”, *Medical Image Analysis 70:1–10*, 2021.
- [8] F. R. Schwartz, D. P. Clark, Y. Ding, J. C. Ramirez-Giraldo, C. T. Badea, D. Marin, “Evaluating renal lesions using **deep-learning based extension** of dual-energy FoV in dual-source CT—A retrospective pilot study”, *European Journal of Radiology 139:109734*, 2021.
- [9] Y. Li, X. Tie, K. Li, J. W. Garrett, G.-H. Chen, “Deep-En-Chroma: **mining the spectral fingerprints in single-kV CT acquisitions using energy integration detectors**”, *SPIE Medical Imaging 2022*.

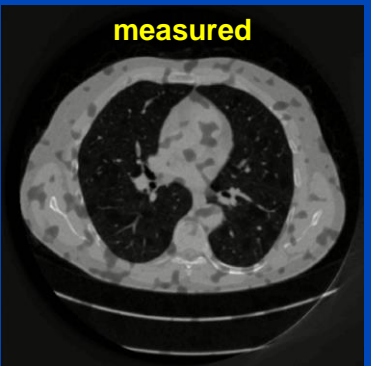
**Real DECT
(ground truth)**

70 kV



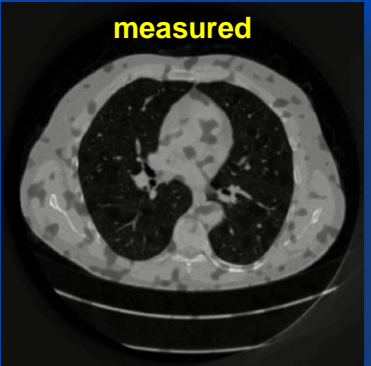
**Fake DECT
(often proposed)**

150 kV Sn

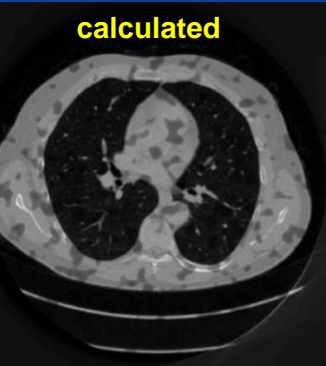
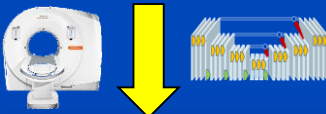
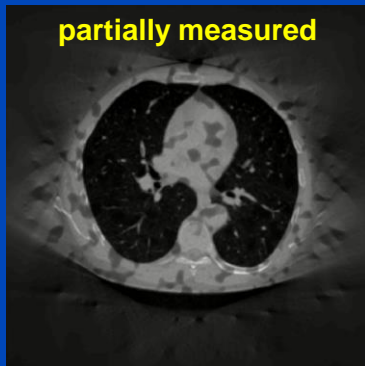


No physical information is available at 150 kV.

final 150 kV Sn

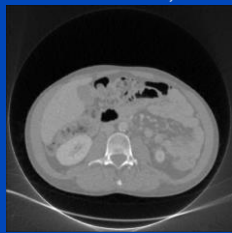


**Partial DECT
(small B FOM)**



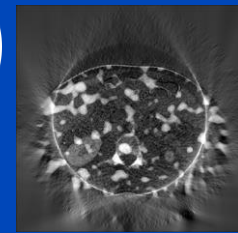
Algorithm for Partial DECT

$$f_0 = f_{,70}$$

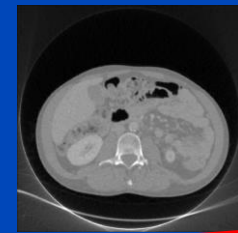


$$\mathbf{X}_s^{-1} \left(\frac{\mathbf{X}_s f_i - p_{s,150}}{\mathbf{X}_s \mathbf{X}_s^{-1} \mathbf{1}} \right)$$

$$u_i$$



$$f_i$$



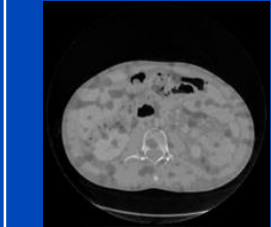
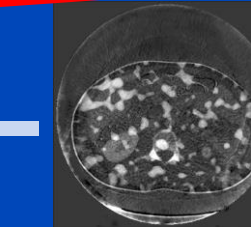
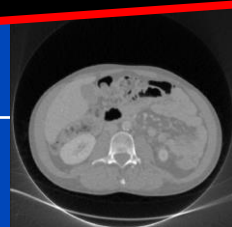
$$\mathbf{X}^T \mathbf{1}$$

$$f_{i+1} = f_i - \text{UNet}(u_i, f_i, \mathbf{X}^T \mathbf{1})$$

Conclusion:

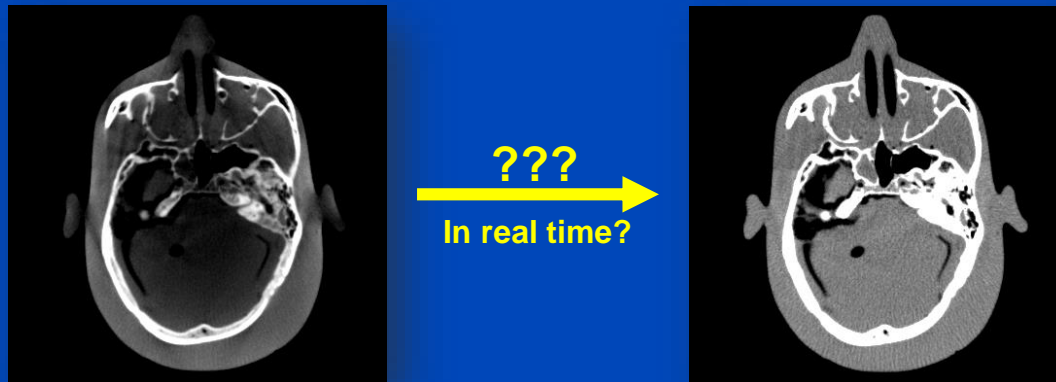
Measuring the physical properties of the patient at more than one energy cannot be avoided!

$$f_{GT}$$



$$L = \|w \cdot (f_i - \text{UNet}_i(u_i, f_i, \mathbf{X}^T \mathbf{1}) - f_{GT})\|^2$$

Deep Scatter Estimation



Monte Carlo Scatter Estimation

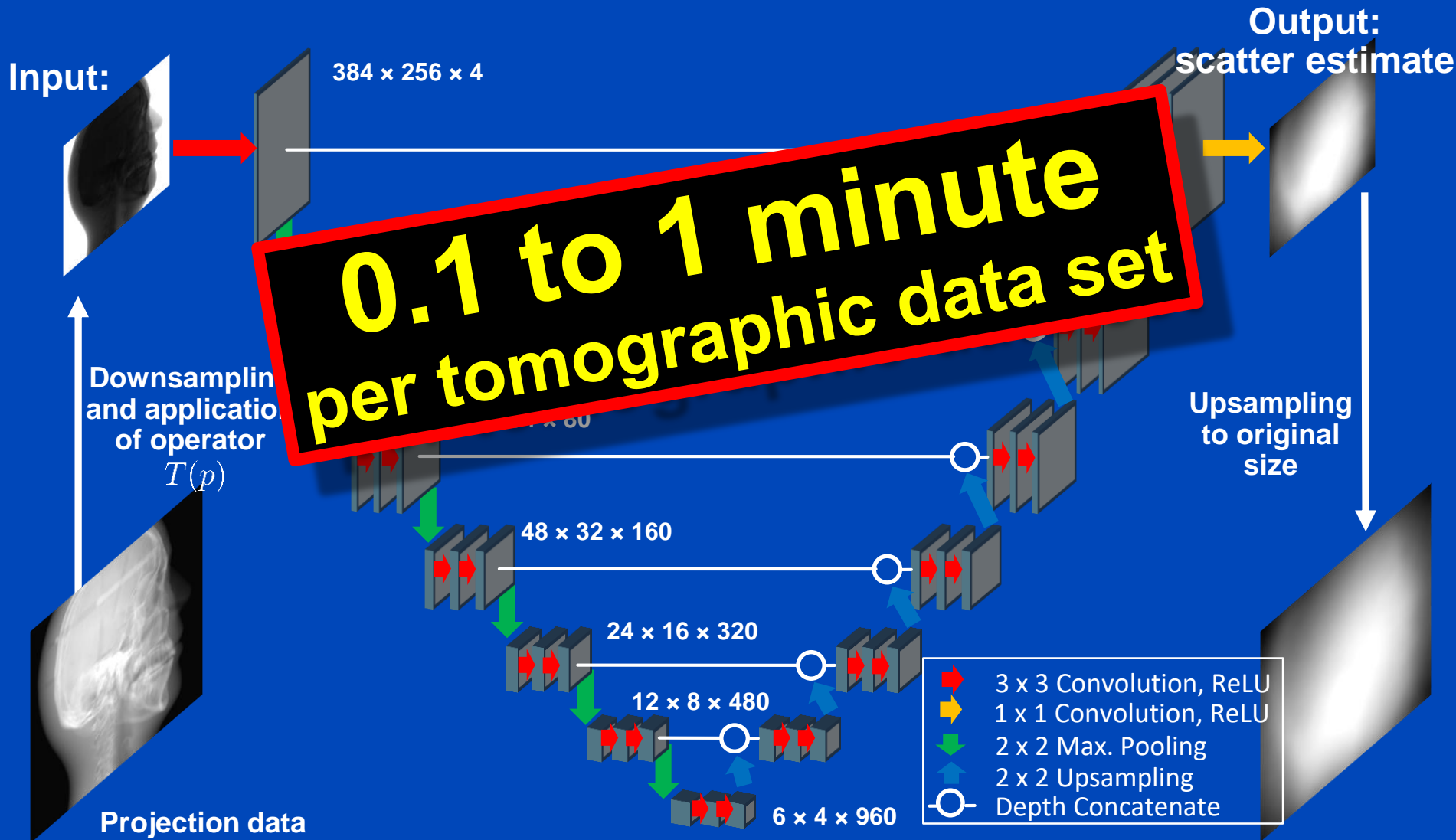
- Simulation of photon trajectories according to physical interaction probabilities.
- Simulating a large number of trajectories well approximates the complete scatter distribution

1 to 10 hours
per tomographic data set



Deep Scatter Estimation

Network architecture & scatter estimation framework



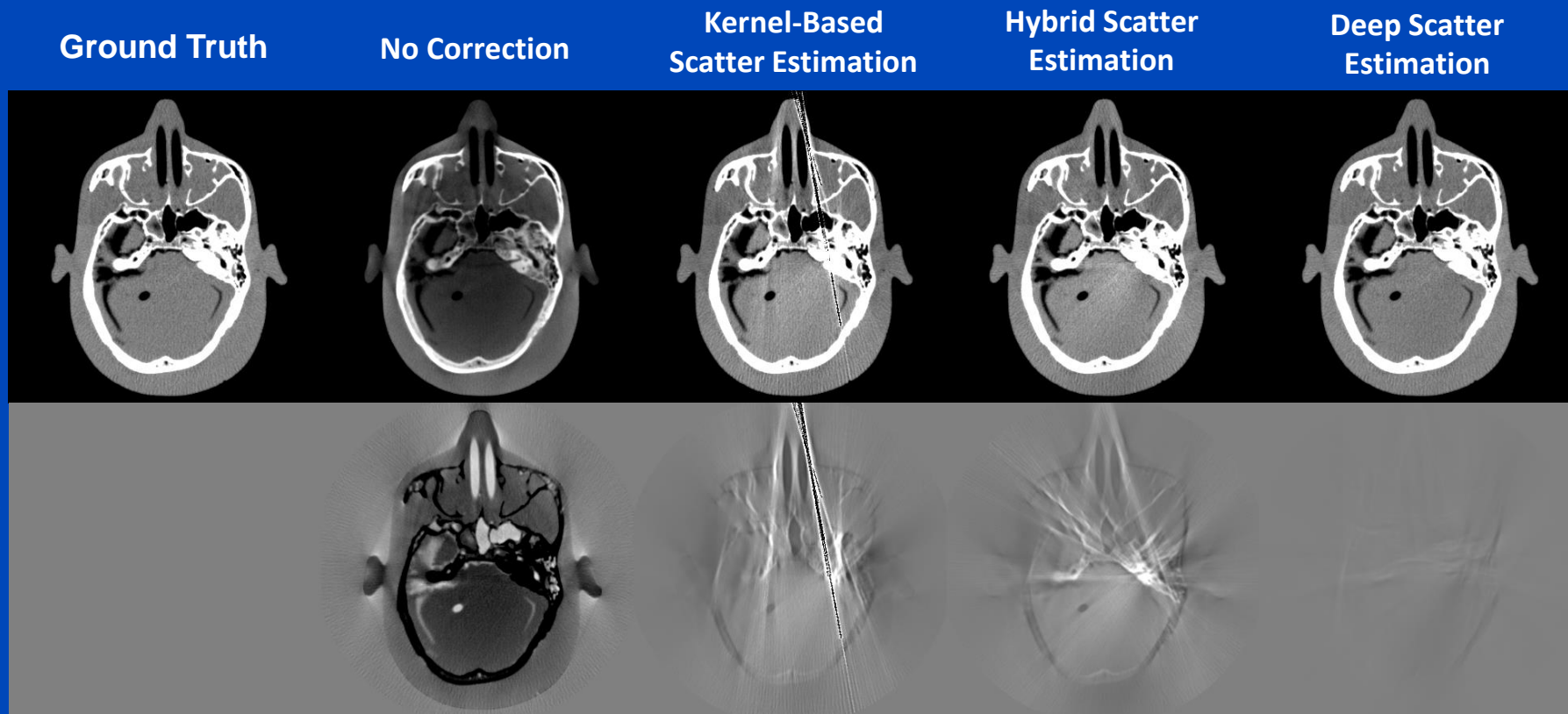
Results on Simulated Projection Data

	Primary intensity	Scatter ground truth (GT)	(Kernel – GT) / GT	(Hybrid - GT) / GT	(DSE – GT) / GT
View #1			14.1% mean absolute percentage error over all projections	7.2% mean absolute percentage error over all projections	1.2% mean absolute percentage error over all projections
View #2					
View #3					
View #4					
View #5			C = 0.5, W = 1.0	C = 0.04, W = 0.04	C = 0 %, W = 50 %

DSE trained to estimate scatter from **primary plus scatter**: High accuracy

Reconstructions of Simulated Data

Difference to ideal CT Reconstruction
simulation



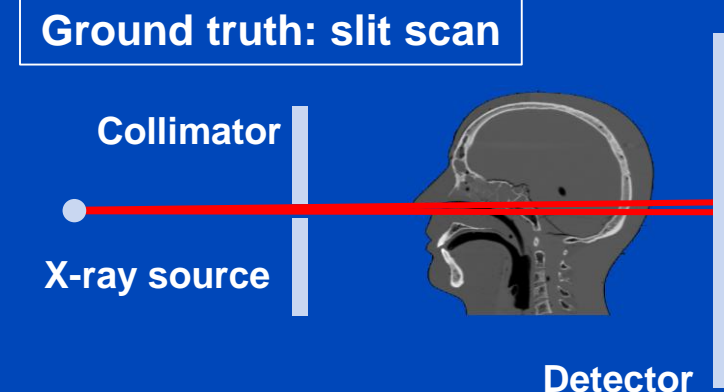
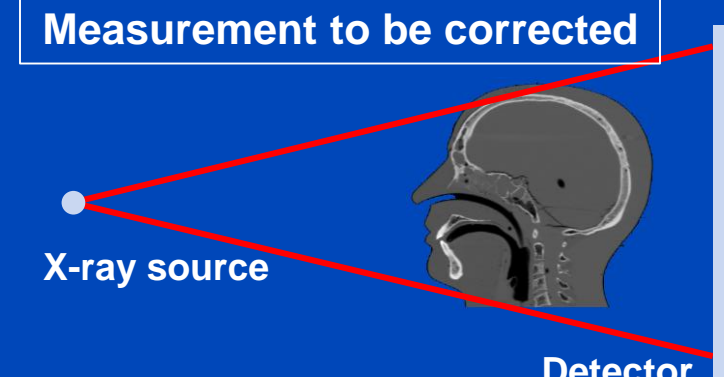
$$C = 0 \text{ HU}, W = 1000 \text{ HU}$$

Testing of the DSE Network for Measured Data (120 kV)

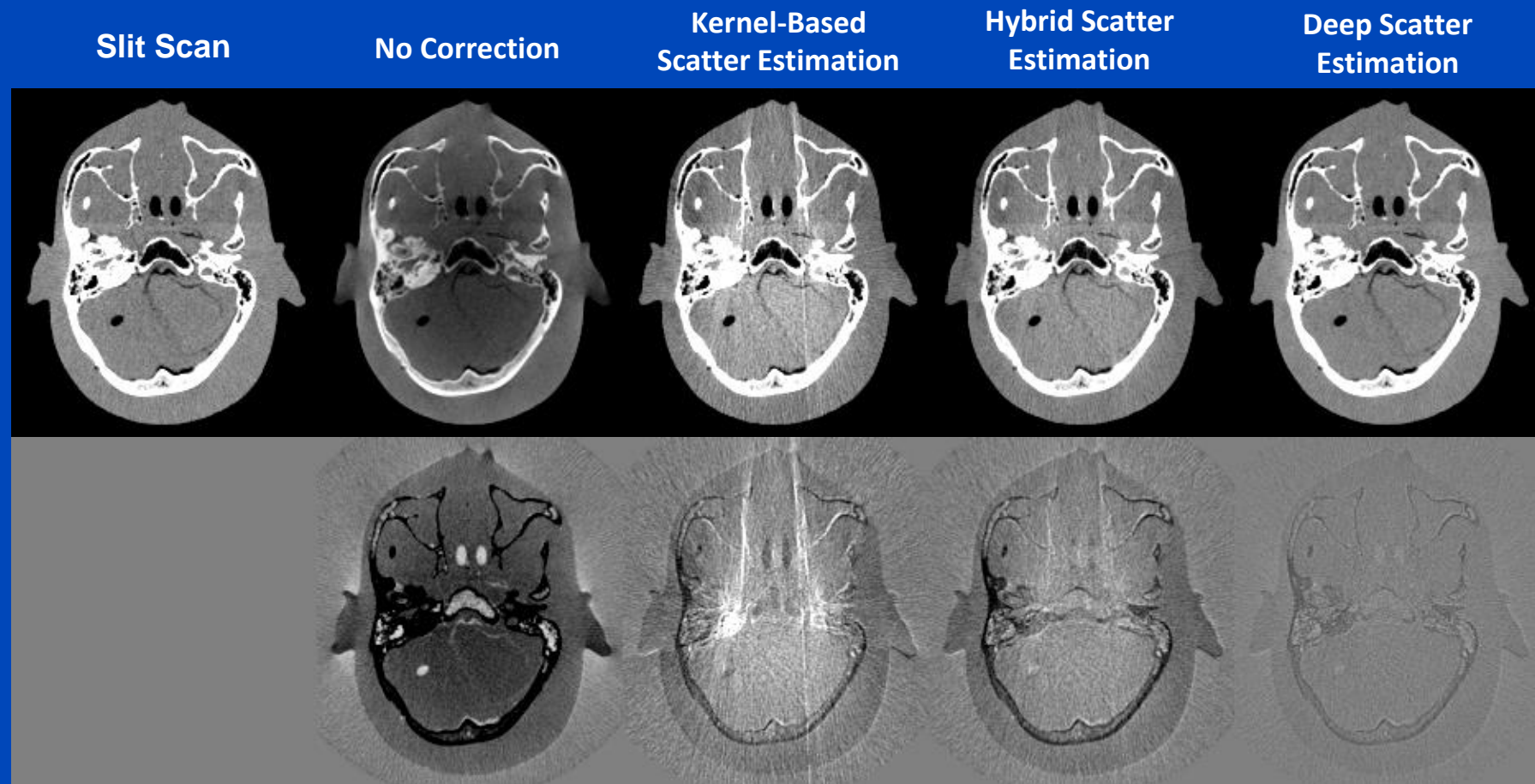
DKFZ table-top CT



- Measurement of a head phantom at our in-house table-top CT.
- Slit scan measurement serves as ground truth.



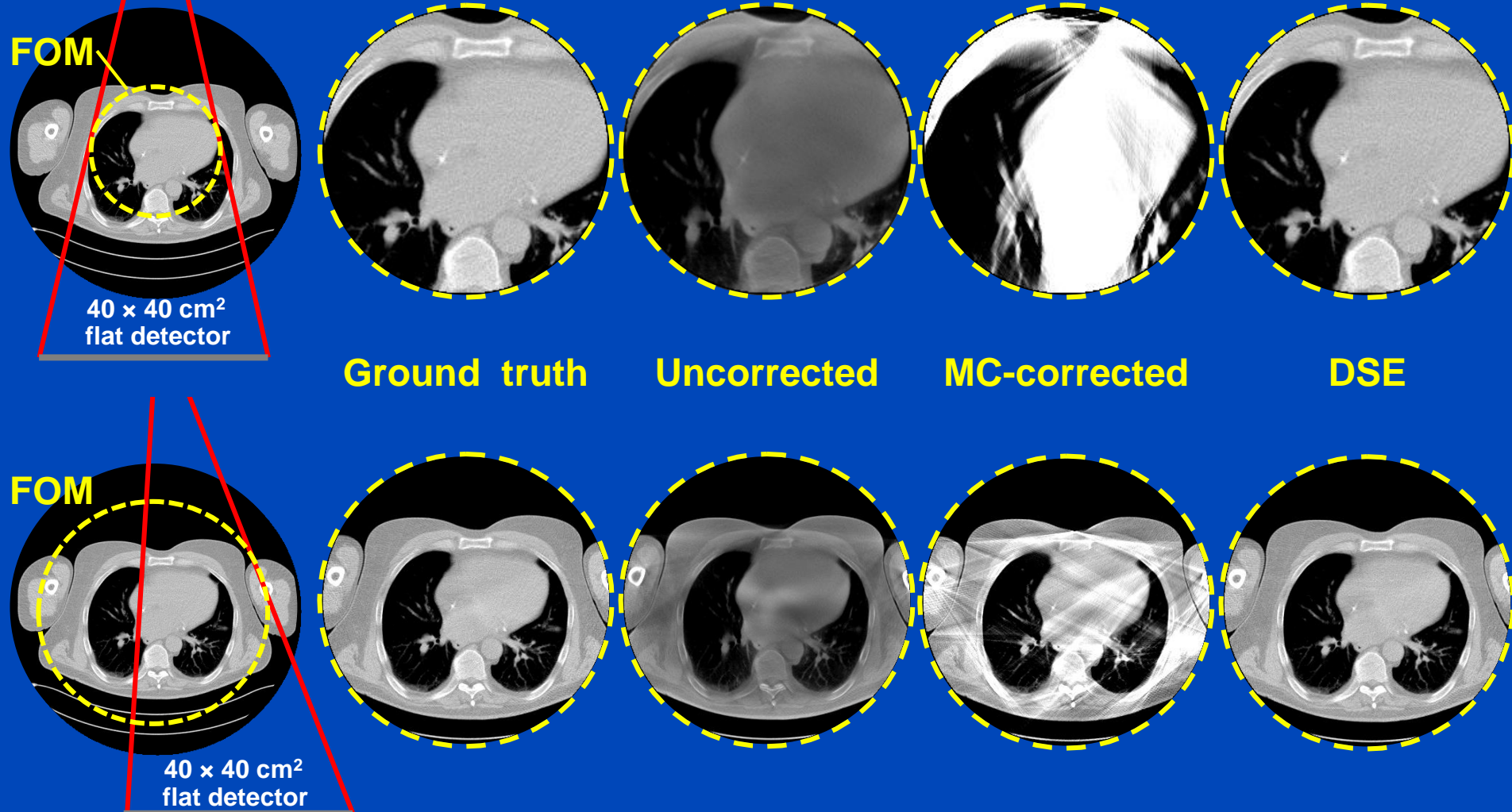
Reconstructions of Measured Data



$$C = 0 \text{ HU}, W = 1000 \text{ HU}$$

A simple detruncation was applied to the rawdata before reconstruction. Images were clipped to the FOM before display. C = -200 HU, W = 1000 HU.

Truncated DSE^{1,2}

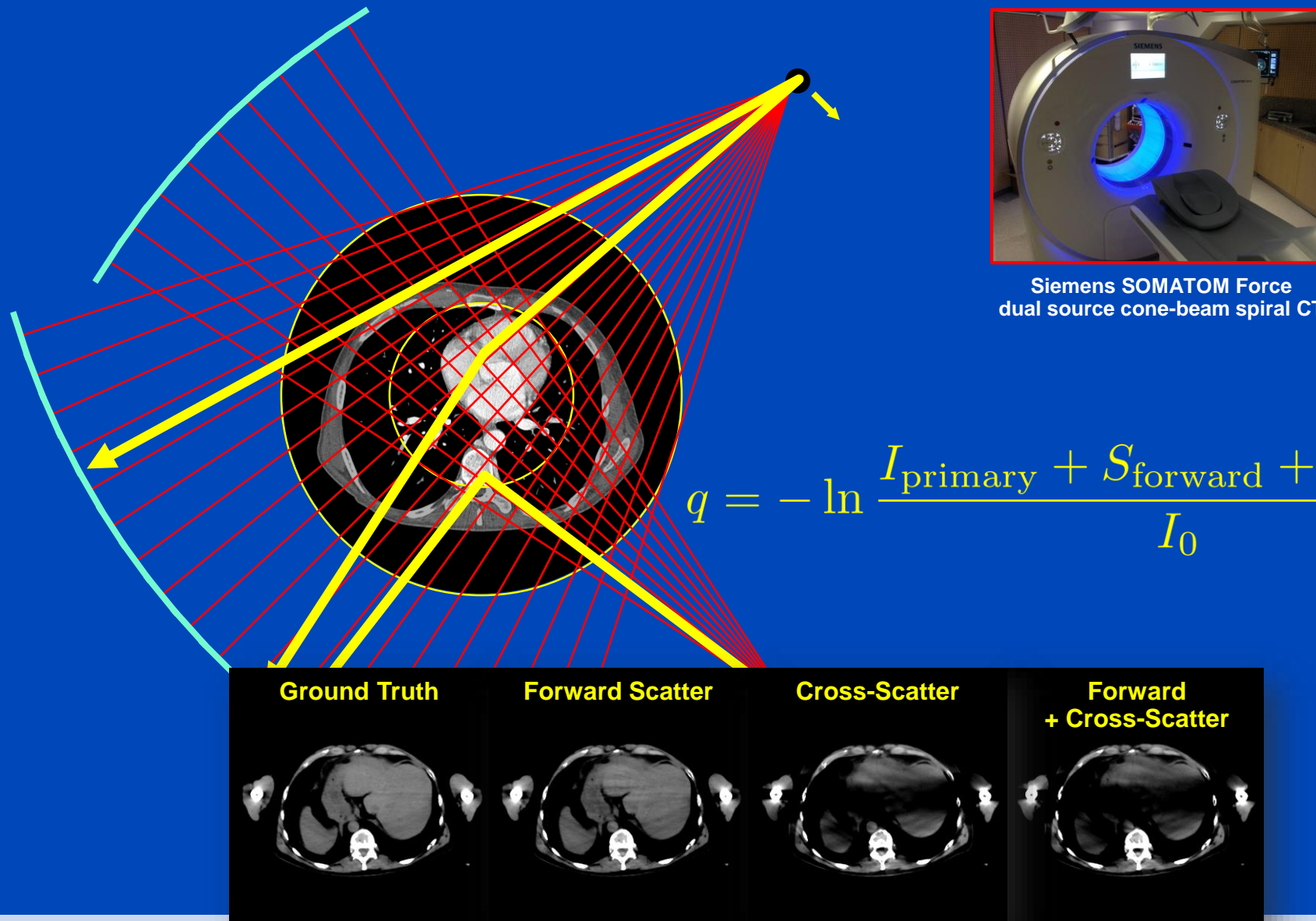


To learn why MC fails at truncated data and what significant efforts are necessary to cope with that situation see [Kachelrieß et al. Effect of detruncation on the accuracy of MC-based scatter estimation in truncated CBCT. Med. Phys. 45(8):3574-3590, August 2018].

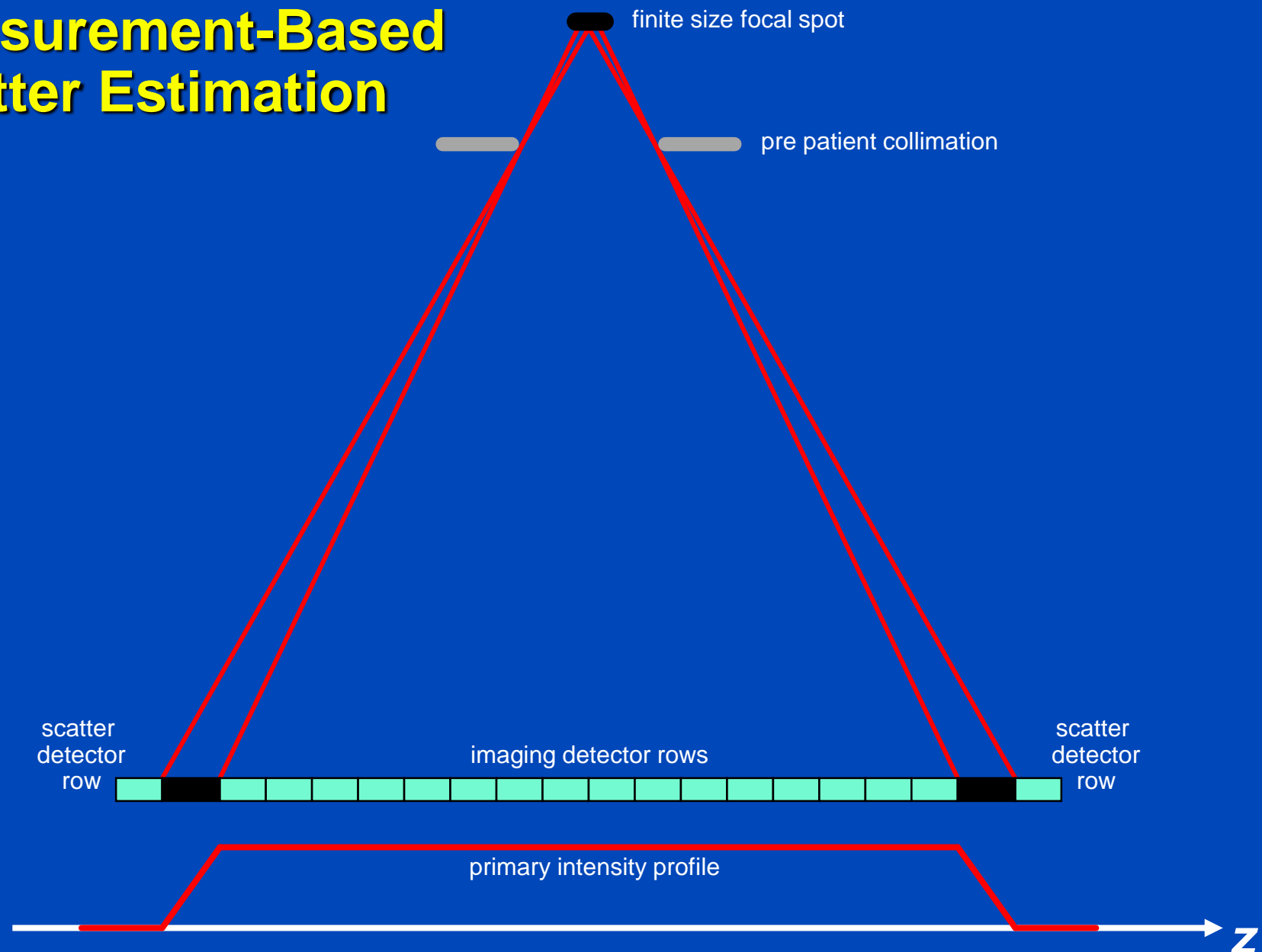
¹J. Maier, M. Kachelrieß et al. Deep scatter estimation (DSE) for truncated cone-beam CT (CBCT). RSNA 2018.

²J. Maier, M. Kachelrieß et al. Robustness of DSE. Med. Phys. 46(1):238-249, January 2019.

Scatter in Dual Source CT (DSCT)



Measurement-Based Scatter Estimation



Cross-DSE

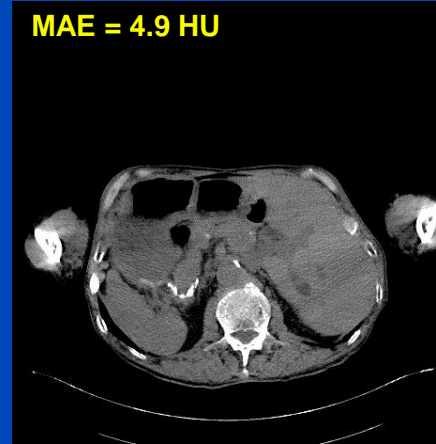
Ground Truth



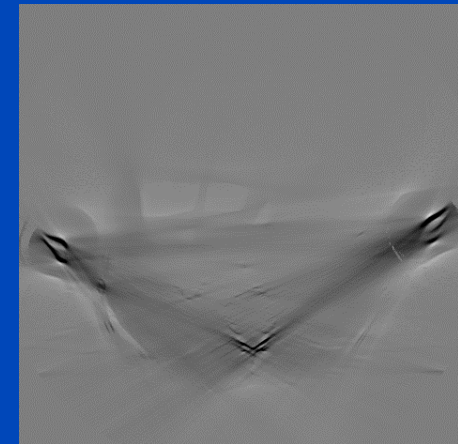
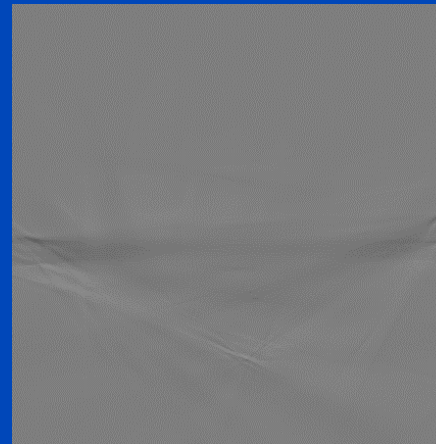
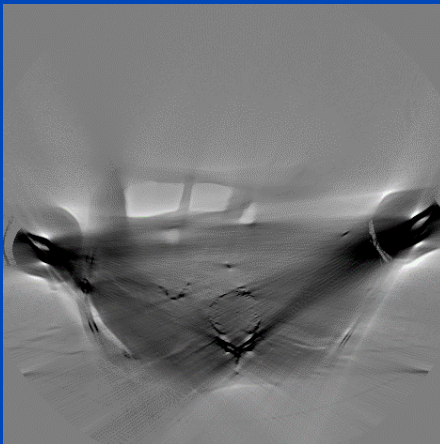
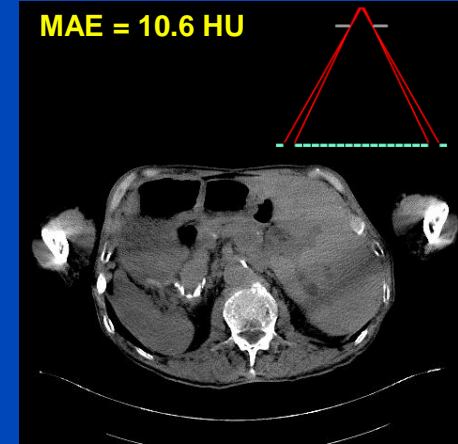
Uncorrected



xDSE (2D, xSSE)



Measurement-based



xDSE (2D, xSSE) maps

primary + forward scatter + cross-scatter + cross-scatter approximation → cross-scatter

Images $C = 40 \text{ HU}$, $W = 300 \text{ HU}$, difference images $C = 0 \text{ HU}$, $W = 300 \text{ HU}$

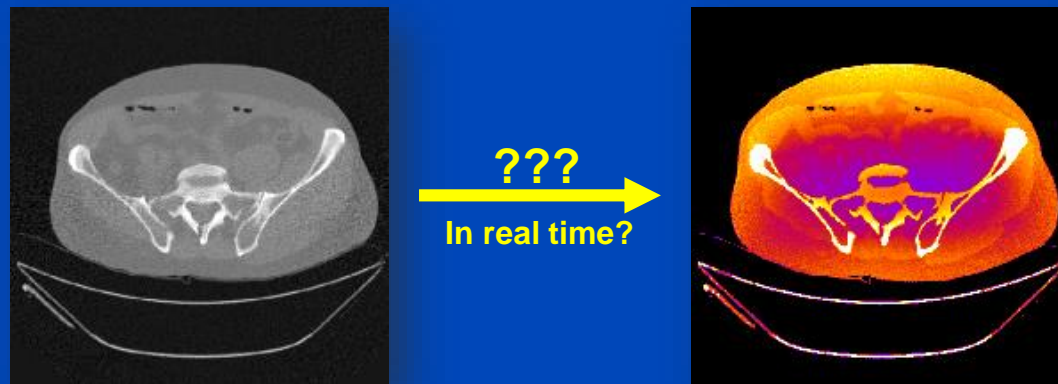
J. Erath, T. Vöth, J. Maier, E. Fournié, M. Petersilka, K. Stierstorfer, and M. Kachelrieß. Deep learning-based forward and cross-scatter correction in dual source CT. Med. Phys. 48:4824–4842, July 2021.

Conclusions on DSE

- DSE needs about 3 ms per CT and 10 ms per CBCT projection (as of 2020).
- DSE is a fast and accurate alternative to MC simulations.
- Facts:
 - DSE can estimate scatter from a single (!) x-ray image.
 - DSE generalizes to all anatomical regions.
 - DSE works for geometries and beam qualities differing from training.
 - DSE may outperform MC even though DSE is trained with MC.
- DSE is not restricted to reproducing MC scatter estimates.

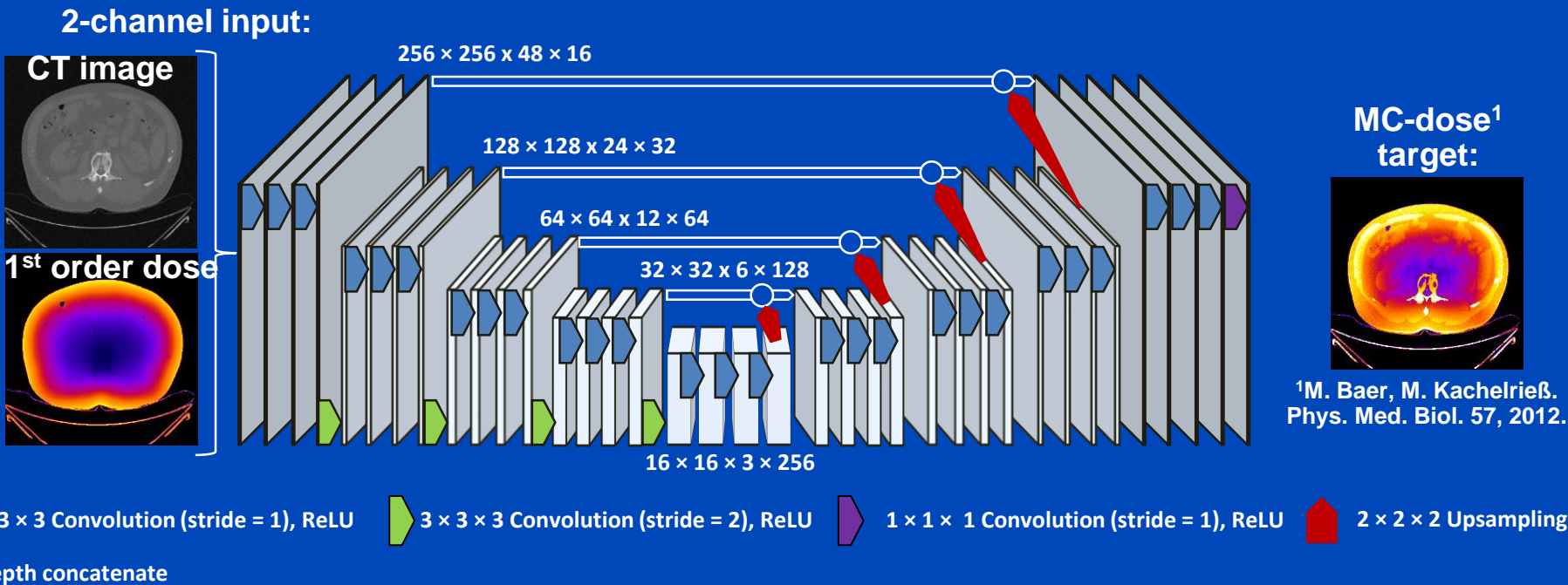
Interested in DSE for photon counting CT?
See first talk in session
RPS 2313, Sunday 9:30, Room Z.

Deep Dose Estimation



Deep Dose Estimation (DDE)

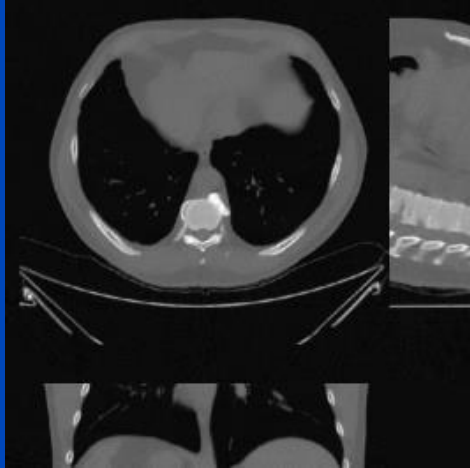
- Combine fast and accurate CT dose estimation using a deep convolutional neural network.
- Train the network to reproduce MC dose estimates given the CT image and a first-order dose estimate.



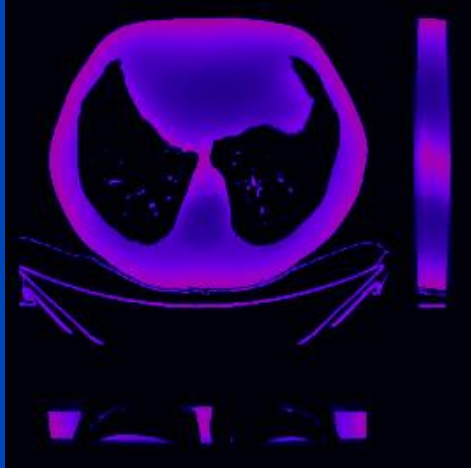
Results

Thorax, tube A, 120 kV, with bowtie

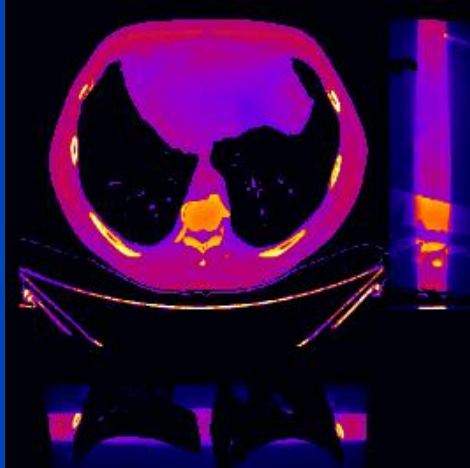
CT image



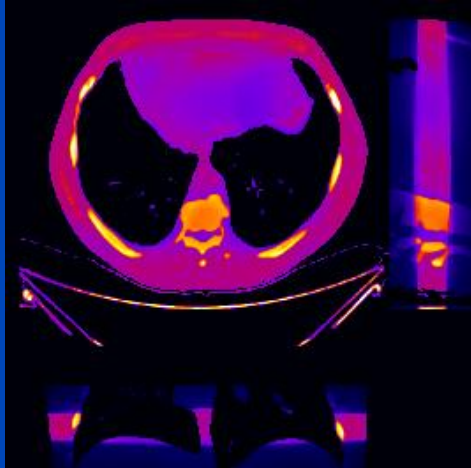
First order dose



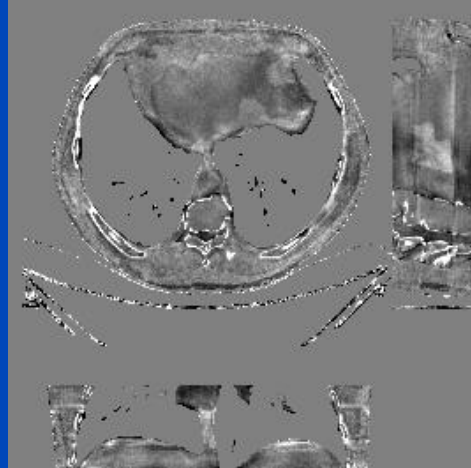
MC ground truth



DDE



Relative error

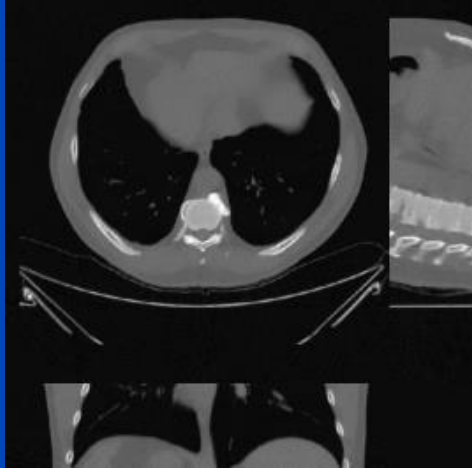


C = 0%
W = 40%

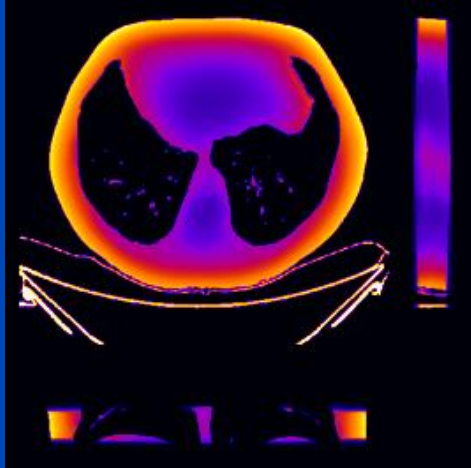
Results

Thorax, tube A, 120 kV, no bowtie

CT image



First order dose

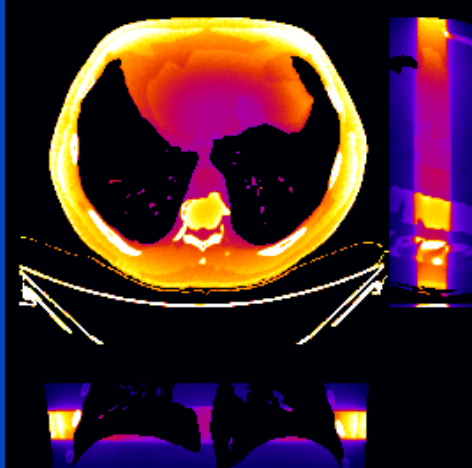


	MC	DDE
48 slices	1 h	0.25 s
whole body	20 h	5 s

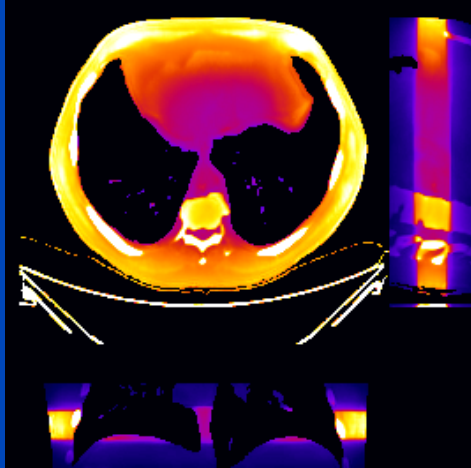
MC uses 16 CPU kernels
DDE uses one Nvidia Quadro P600 GPU

DDE training took 74 h for 300 epochs,
1440 samples, 48 slices per sample

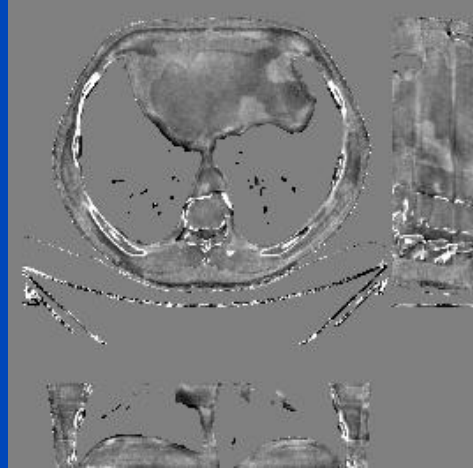
MC ground truth



DDE



Relative error

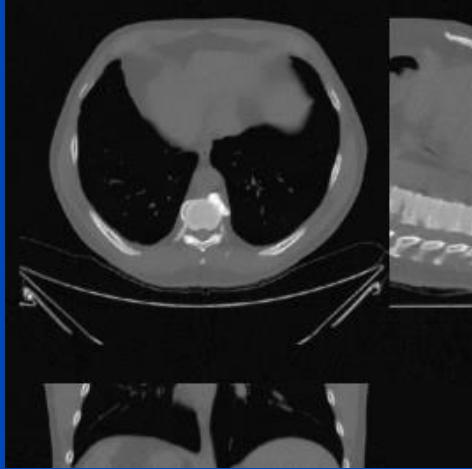


$$C = 0\% \\ W = 40\%$$

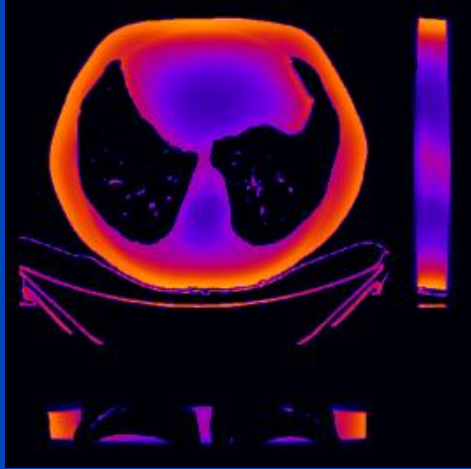
Results

Thorax, tube B, 120 kV, no bowtie

CT image



First order dose

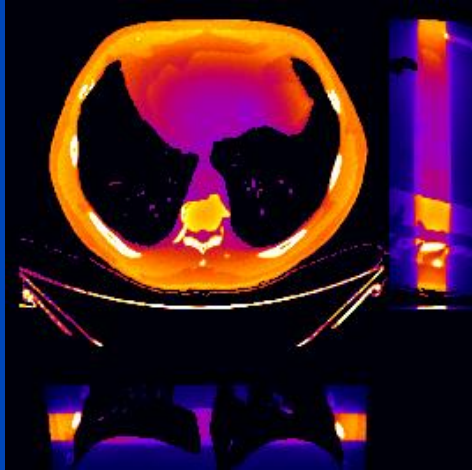


	MC	DDE
48 slices	1 h	0.25 s
whole body	20 h	5 s

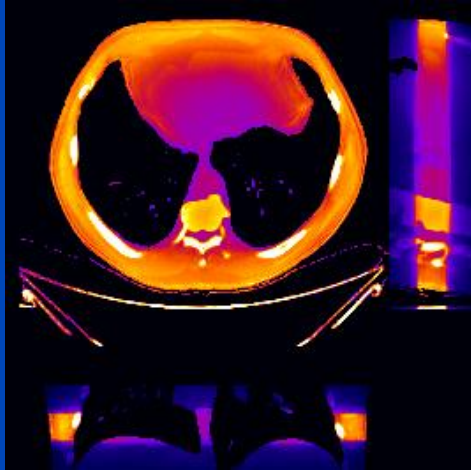
MC uses 16 CPU kernels
DDE uses one Nvidia Quadro P600 GPU

DDE training took 74 h for 300 epochs,
1440 samples, 48 slices per sample

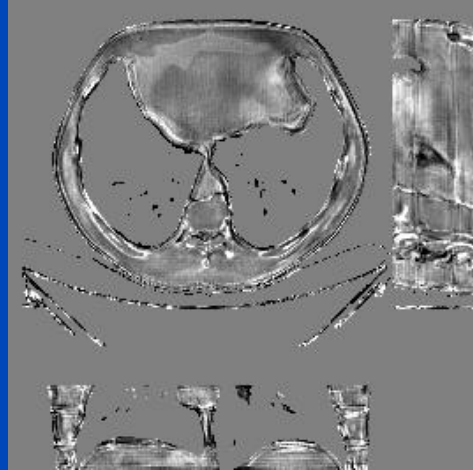
MC ground truth



DDE



Relative error



C = 0%
W = 40%

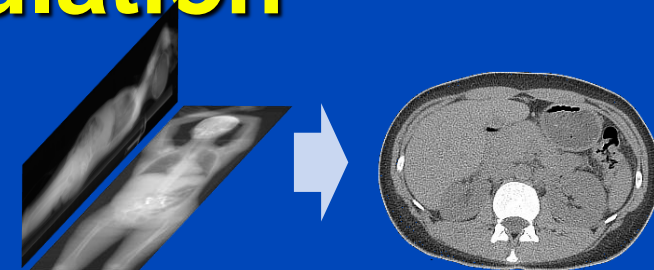
Conclusions on DDE

- DDE provides accurate dose predictions
 - for circle scans
 - for sequence scans
 - for partial scans (less than 360°)
 - for limited angle scans (less than 180°)
 - for spiral scans
 - for different tube voltages
 - for scans with and without bowtie filtration
 - for scans with tube current modulation
- In practice it may therefore be not necessary to perform separate training runs for these cases.
- Thus, accurate real-time patient dose estimation may become feasible with DDE.

Patient Risk-Minimizing Tube Current Modulation

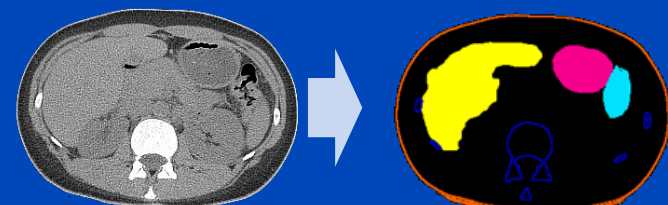
1. Coarse reconstruction from two scout views

- E.g. X. Ying, et al. X2CT-GAN: Reconstructing CT from biplanar x-rays with generative adversarial networks. CVPR 2019.



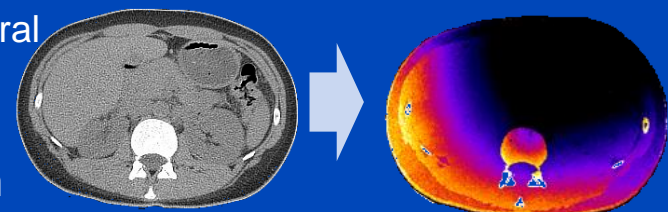
2. Segmentation of radiation-sensitive organs

- E.g. S. Chen, M. Kachelrieß et al., Automatic multi-organ segmentation in dual-energy CT (DECT) with dedicated 3D fully convolutional DECT networks. Med. Phys. 2019.



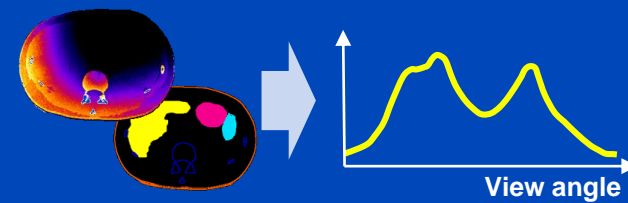
3. Calculation of the effective dose per view using the deep dose estimation (DDE)

- J. Maier, E. Eulig, S. Dorn, S. Sawall and M. Kachelrieß. Real-time patient-specific CT dose estimation using a deep convolutional neural network. IEEE Medical Imaging Conference Record, M-03-178: 3 pages, Nov. 2018.



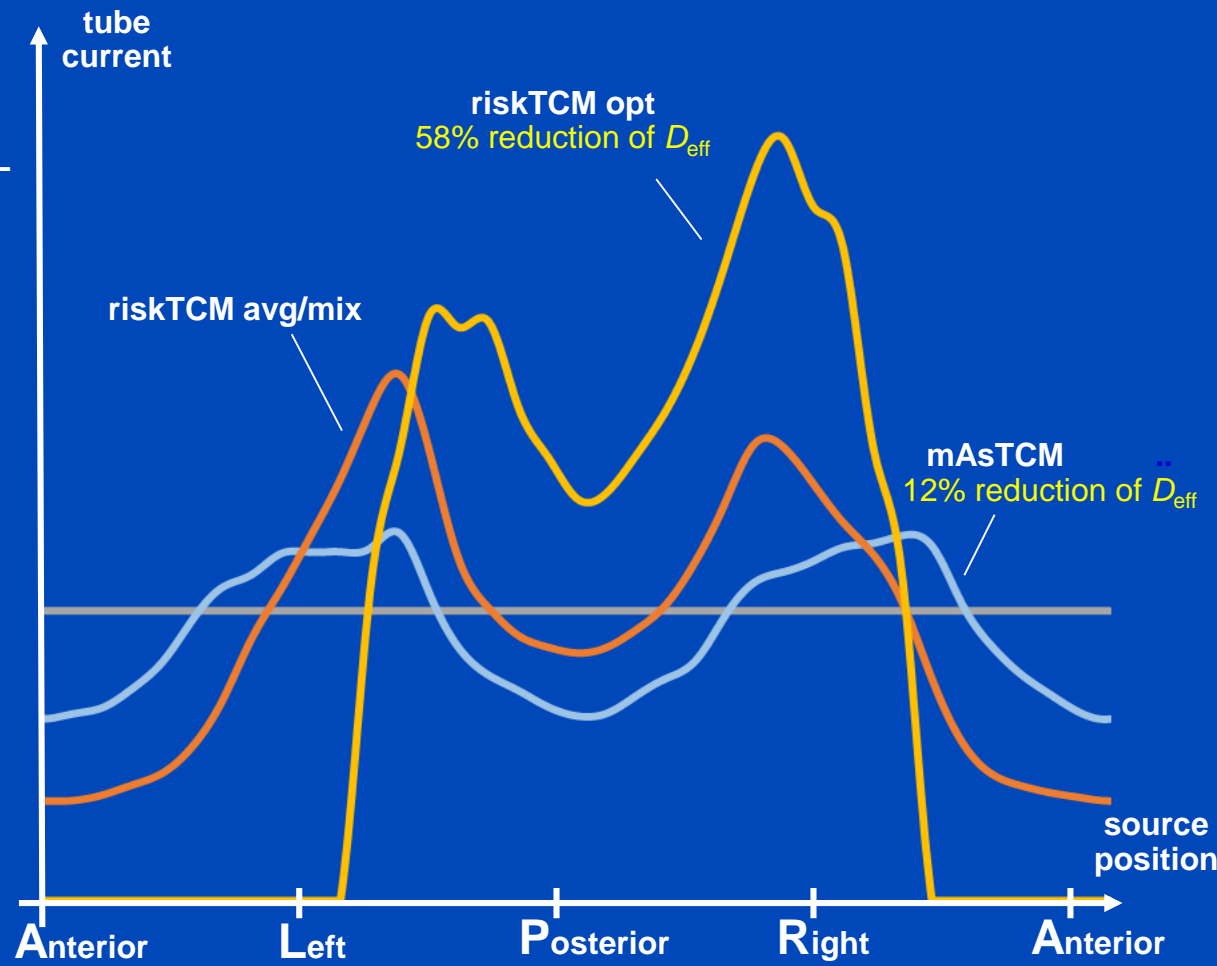
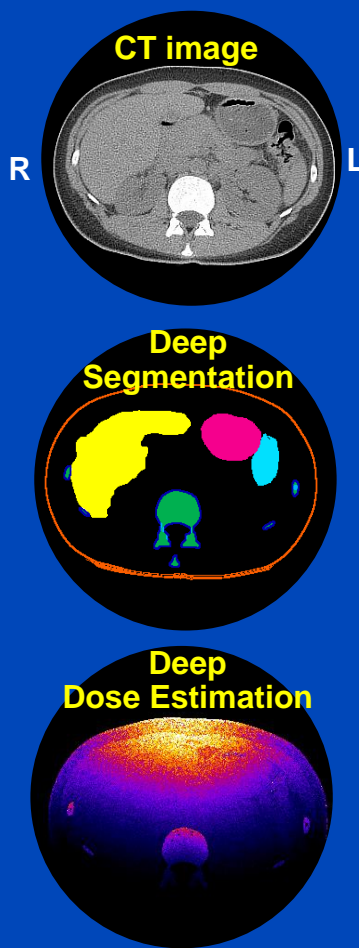
4. Determination of the tube current modulation curve that minimizes the radiation risk

- L. Klein, C. Liu, J. Steidel, L. Enzmann, M. Knaup, S. Sawall, A. Maier, M. Lell, J. Maier, and M. Kachelrieß. Patient-specific radiation risk-based tube current modulation for diagnostic CT. Med. Phys. 49: in press, 2022.

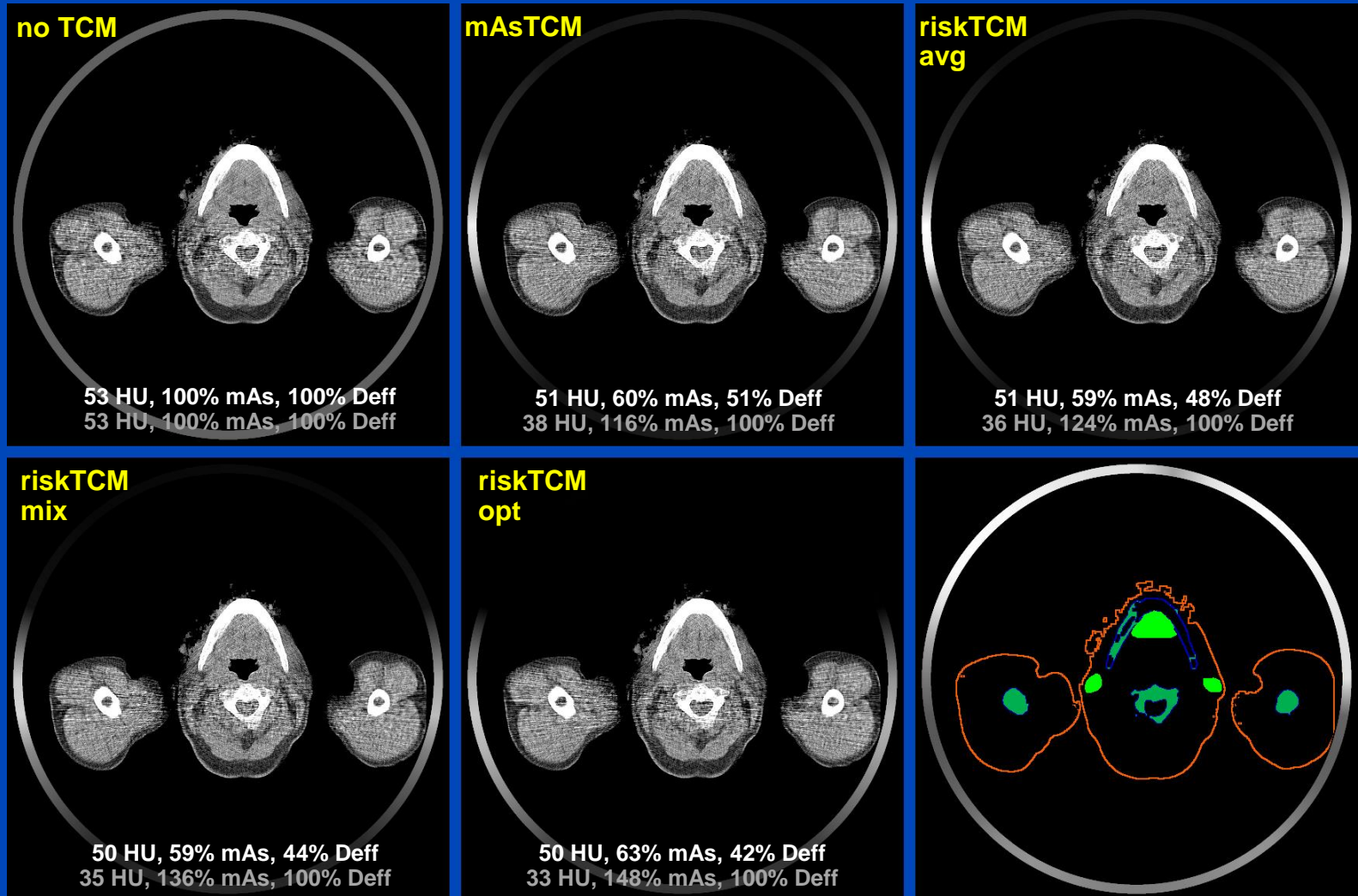


More details see first talk in RPS 1213 Friday 8:00 in Room Z.

Remainder 0.12
Bone surface 0.01
Brain 0.01
Breast 0.12
Colon 0.12
Red Bone Marrow 0.12
Salivary glands 0.01
Esophagus 0.04
Liver 0.04
Lung 0.12
Skin 0.01
Stomach 0.12
Gonads 0.08
Thyroid 0.04
Bladder 0.04



Patient 03 - Neck

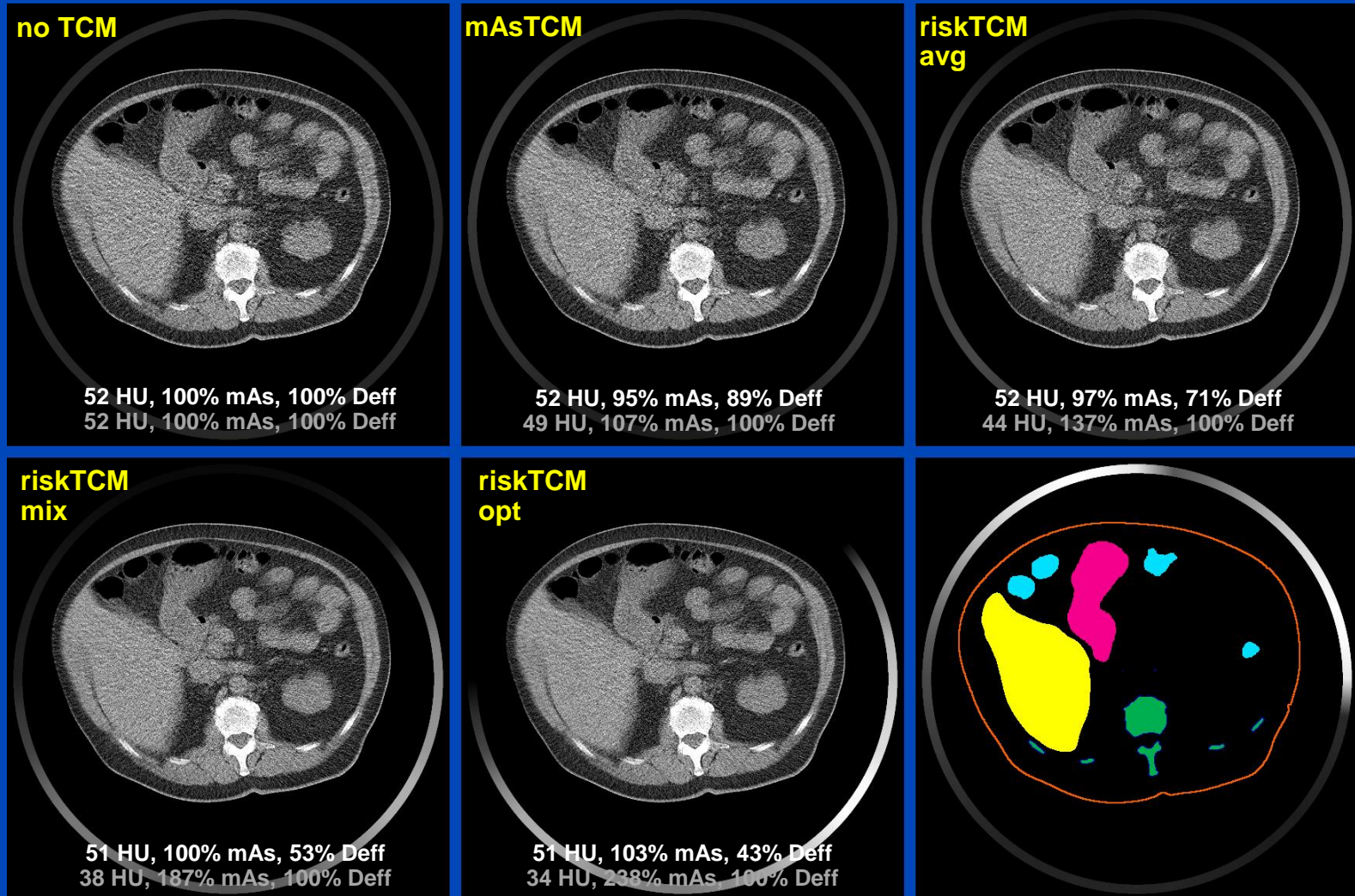


$C = 25 \text{ HU}$, $W = 400 \text{ HU}$

L. Klein, C. Liu, J. Steidel, L. Enzmann, M. Knaup, S. Sawall, A. Maier, M. Lell, J. Maier, and M. Kachelrieß.
Patient-specific radiation risk-based tube current modulation for diagnostic CT. Med. Phys. 49: in press, 2022.

dkfz.

Patient 04 - Abdomen



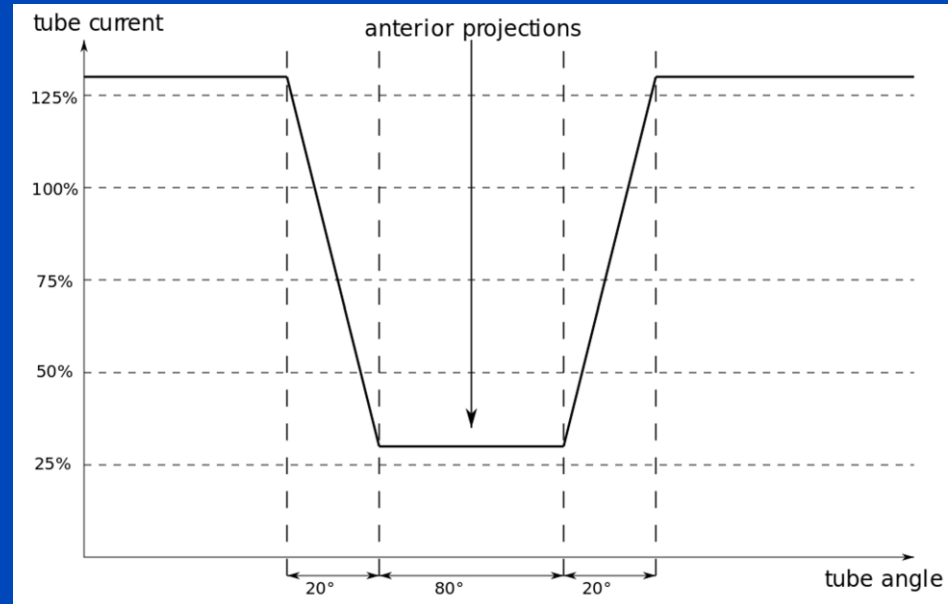
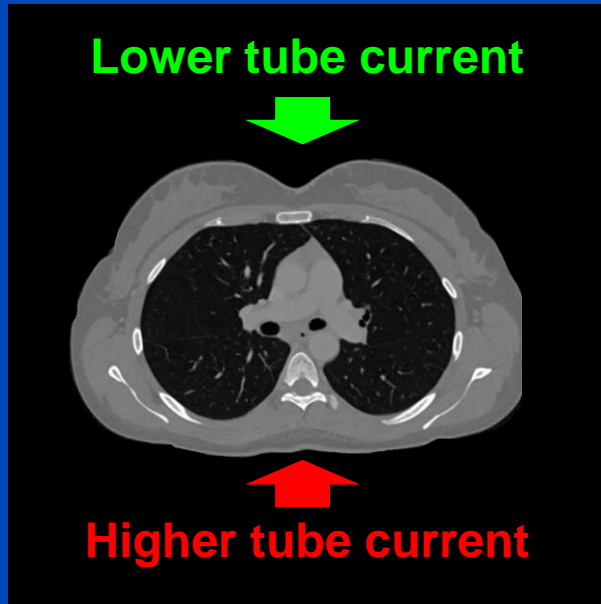
$C = 25 \text{ HU}$, $W = 400 \text{ HU}$

L. Klein, C. Liu, J. Steidel, L. Enzmann, M. Knaup, S. Sawall, A. Maier, M. Lell, J. Maier, and M. Kachelrieß.
Patient-specific radiation risk-based tube current modulation for diagnostic CT. Med. Phys. 49: in press, 2022.

dkfz.

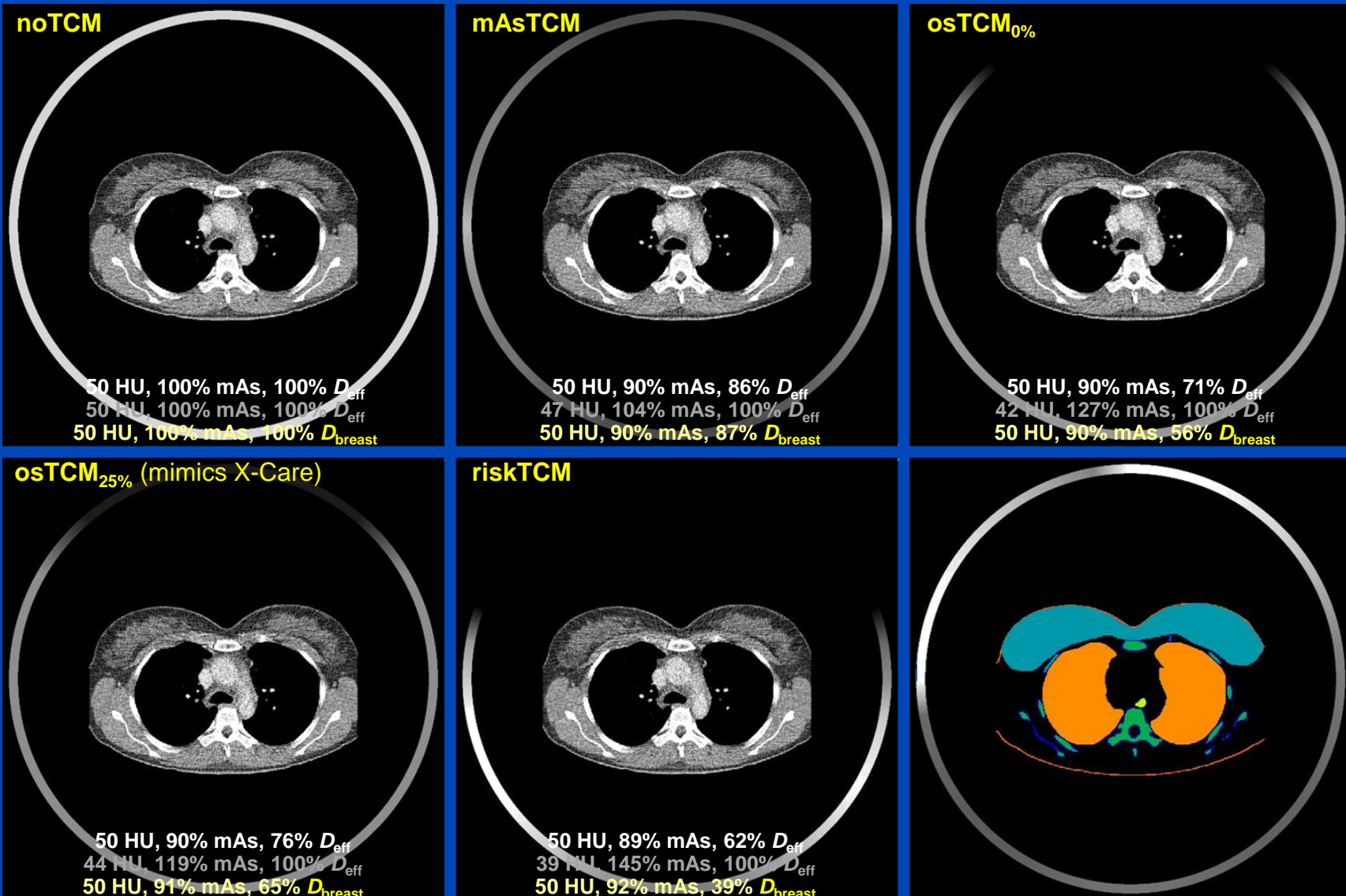
riskTCM vs. Breast-Specific TCM

- osTCM mimics X-Care (Siemens Healthineers)
- Reduces the tube current to 25% for the anterior 120°
- Higher tube current for the remaining 240°



D. Ketelsen et al. Automated computed tomography dosesaving algorithm to protect radiosensitive tissues: estimation of radiation exposure and image quality considerations. Invest Radiol, 47(2):148–52, 2012

Results



Data courtesy of Prof. Lell, Nürnberg. C = 25 HU, W = 400 HU

L. Klein, L. Enzmann, A. Byl, C. Liu, S. Sawall, A. Maier, J. Maier, M. Lell, and M. Kachelrieß.
Organ- vs. patient risk-specific TCM in thorax CT scans covering the female breast. CT Meeting 2022.

Conclusions on RiskTCM

- Risk-specific TCM minimizes the patient risk.
- With D_{eff} as a risk model riskTCM can reduce risk by up to 50% and more, compared with the gold standard mAsTCM.
- Other risk models, in particular age-, weight- and sex-specific models, can be used with riskTCM as well.
- Note:
 - mAsTCM = good for the x-ray tube
 - riskTCM = good for the patient
 - detector flux equalizing TCM = good for the detector

More details see scientific presentation by Klein et al. in session RPS 1213 "Advances in CT dosimetry and radiobiology" Friday 8:00 in Room Z.

ECR 2022 – Best Research Presentation Abstract

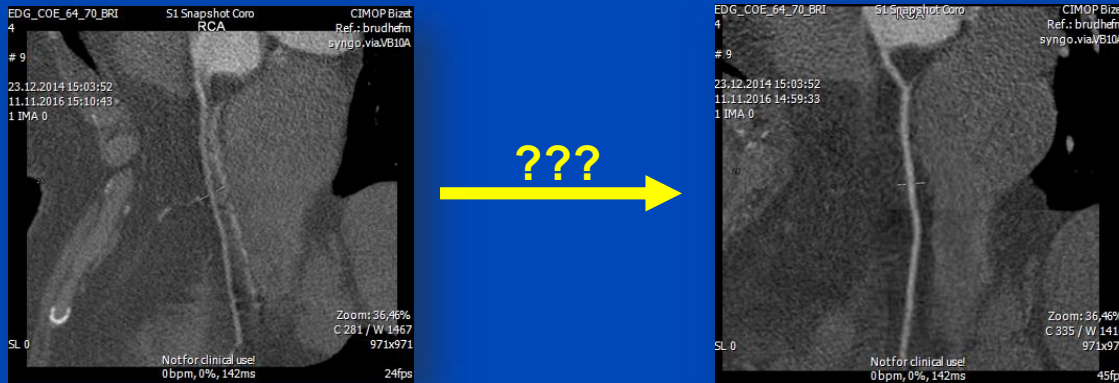
within the topic Physics in Medical Imaging
with the presentation:



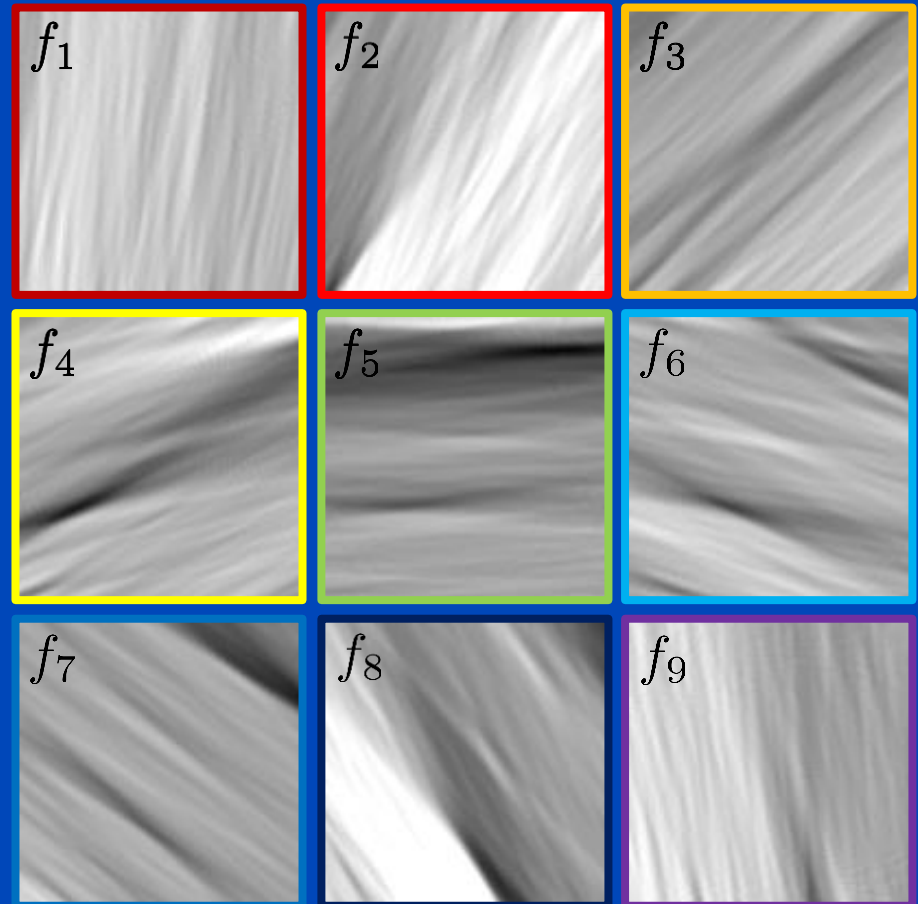
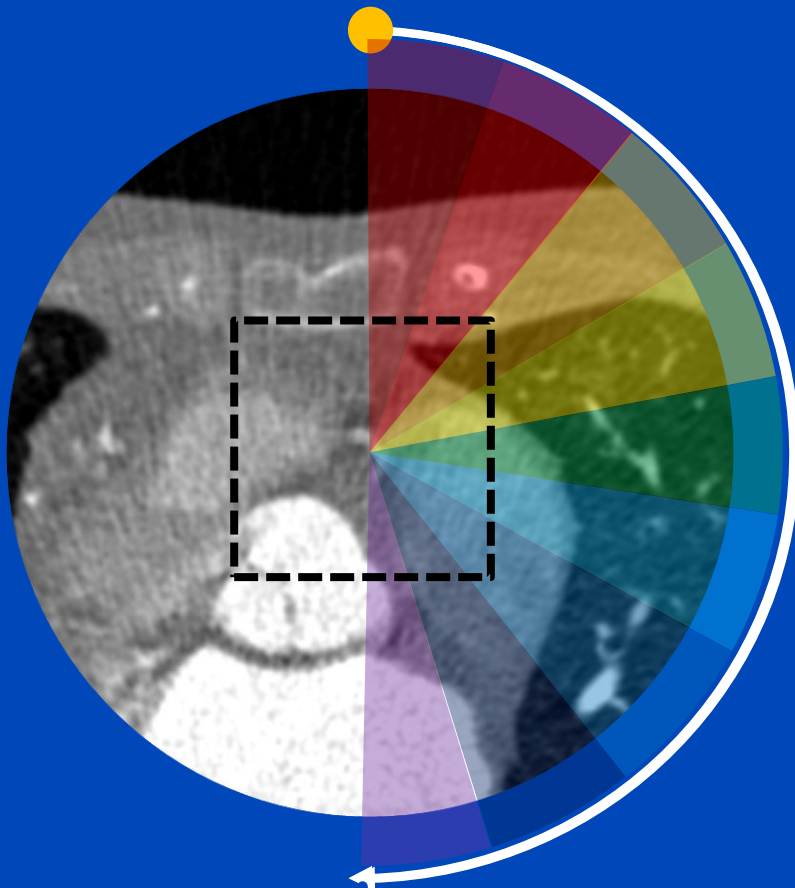
Risk-minimising tube current modulation (riskTCM) for CT – potential dose reduction across different tube voltages (16765)

L. Klein¹, C. Liu², J. Steidel¹, L. Enzmann¹, S. Sawall¹, J. Maier¹, A. Maier², M. Lell³, M. Kachelrieß¹; ¹Heidelberg/DE, ²Erlangen/DE, ³Nuremberg/DE

Deep Cardiac Motion Compensation

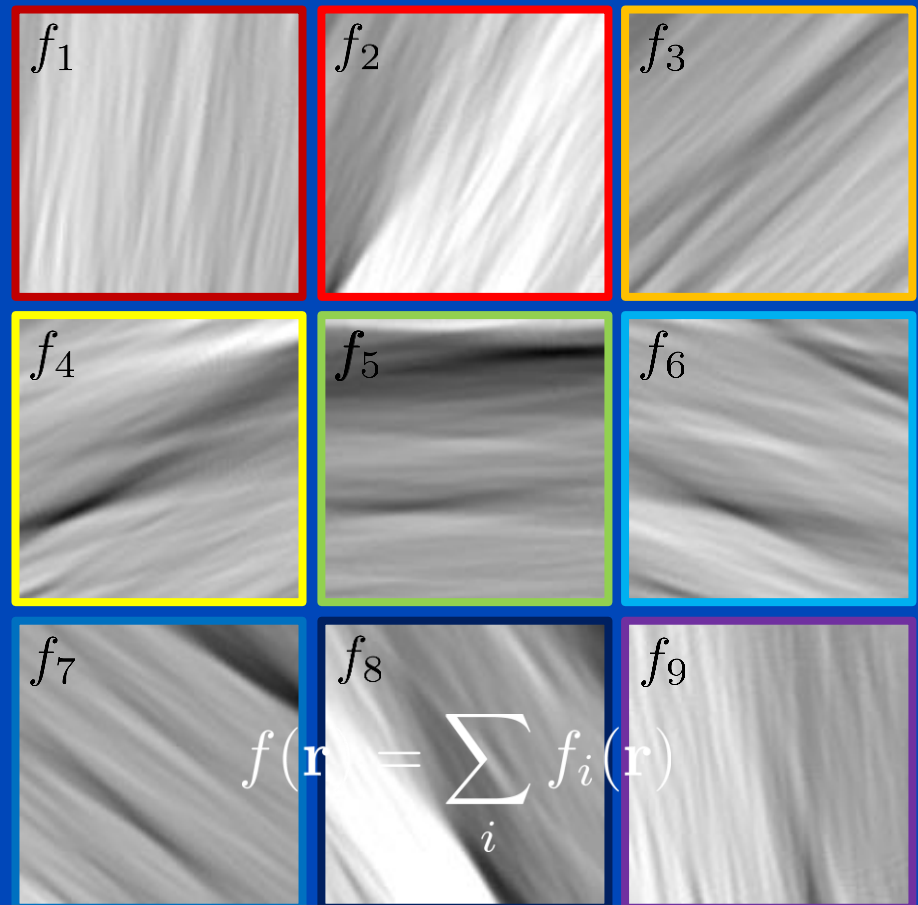
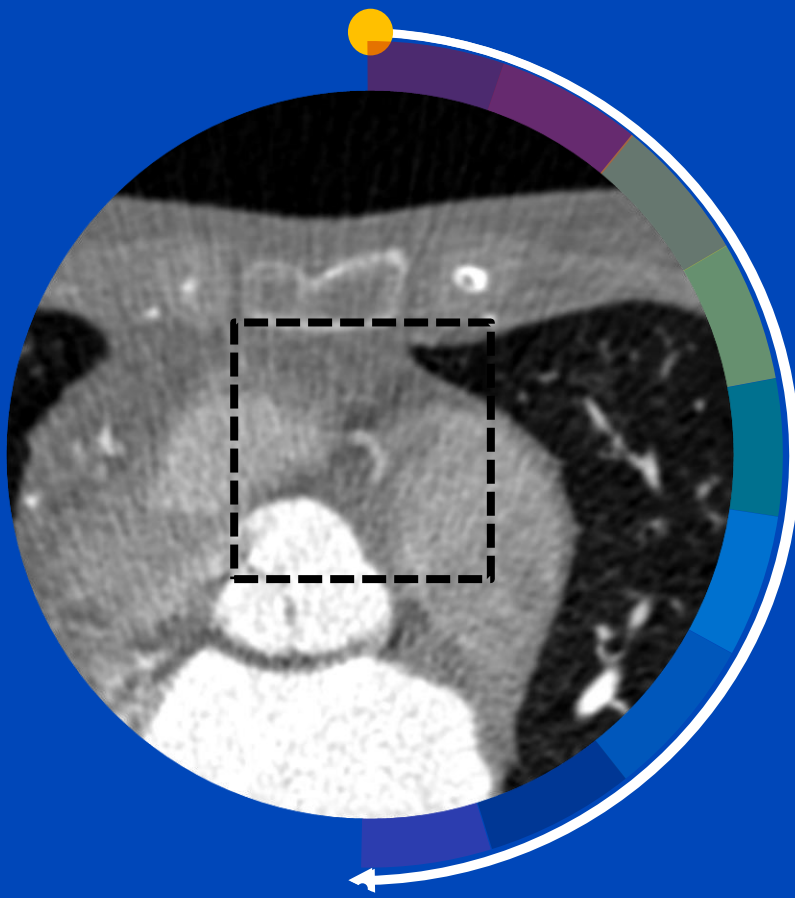


Partial Angle-Based Motion Compensation (PAMoCo)

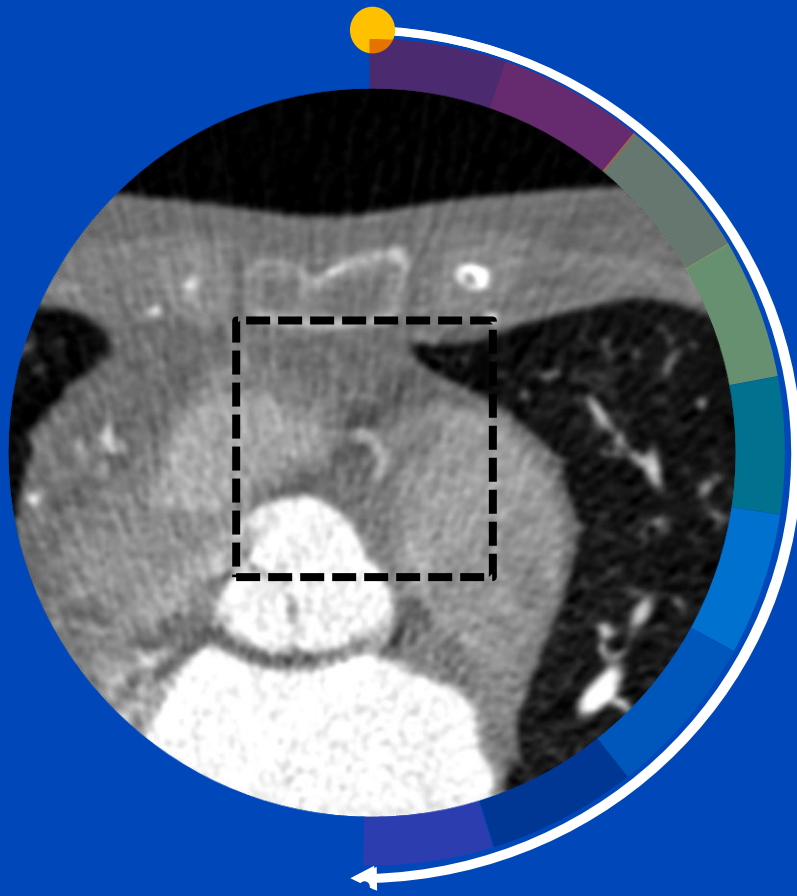


Animated rotation time = 100 × real rotation time

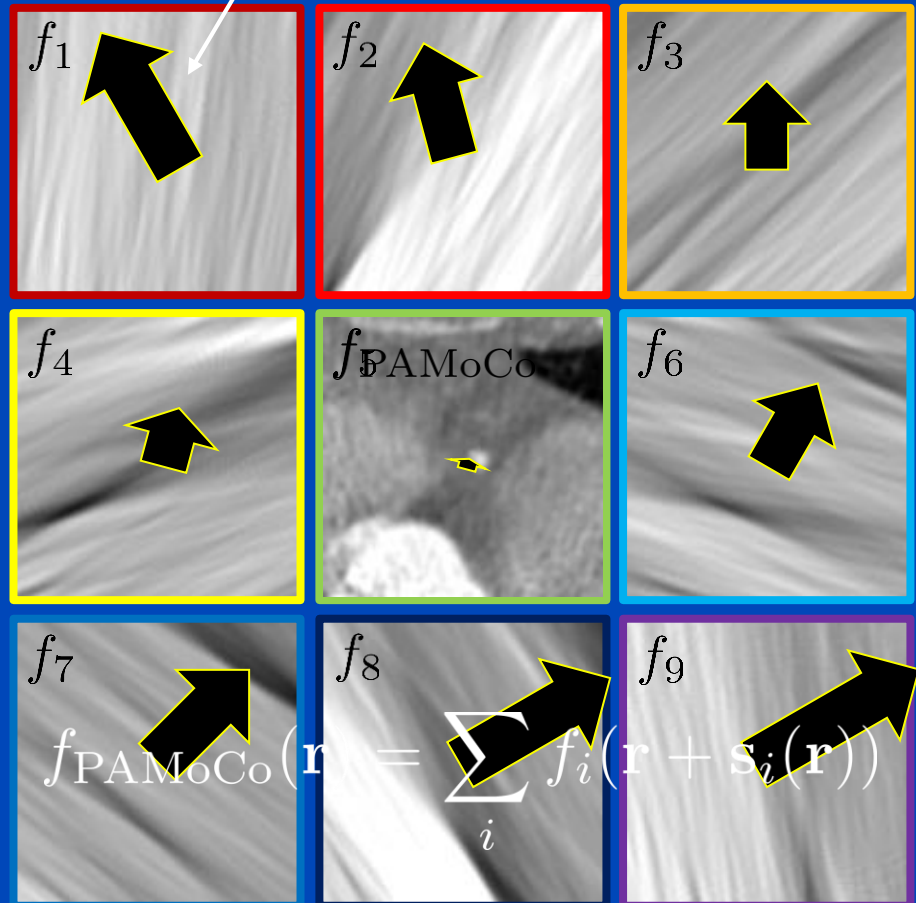
Partial Angle-Based Motion Compensation (PAMoCo)



Partial Angle-Based Motion Compensation (PAMoCo)



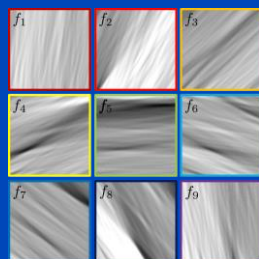
Motion vector field $s_1(\mathbf{r})$



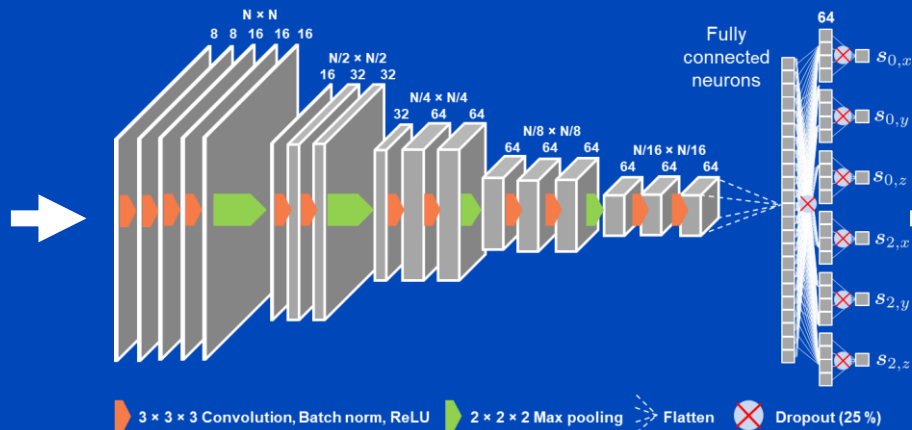
Apply motion vector fields (MVF) to partial angle reconstructions

Deep Partial Angle-Based Motion Compensation (Deep PAMoCo)

PARs centered around coronary artery



Neural network to predict parameters of a motion model

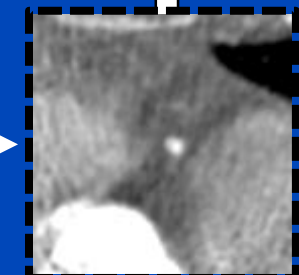


Reinsertion of patch into initial reconstruction



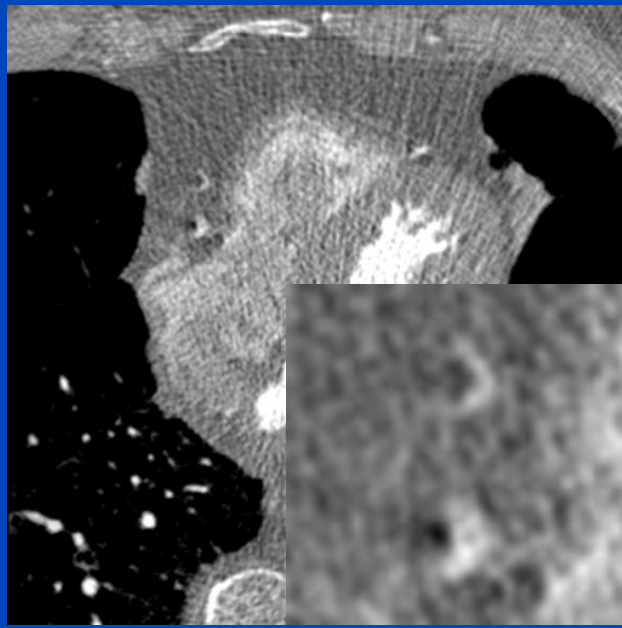
Spatial transformer

Application of the motion model to the PARs via a spatial transformer¹

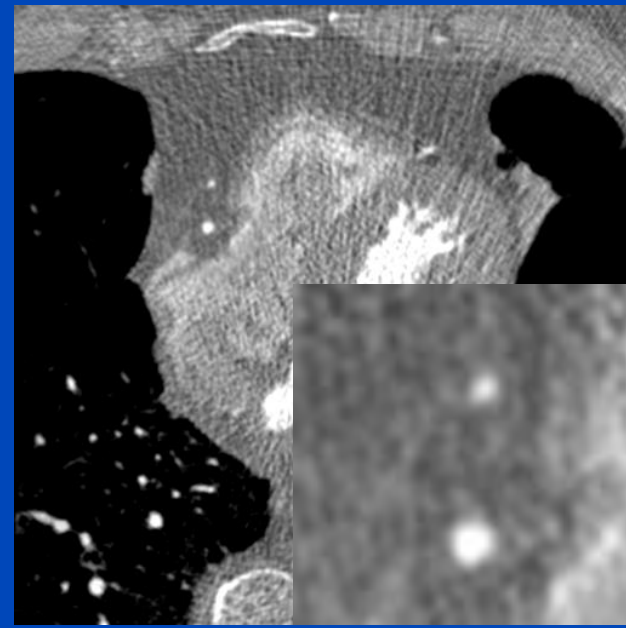


Patient 1

Original



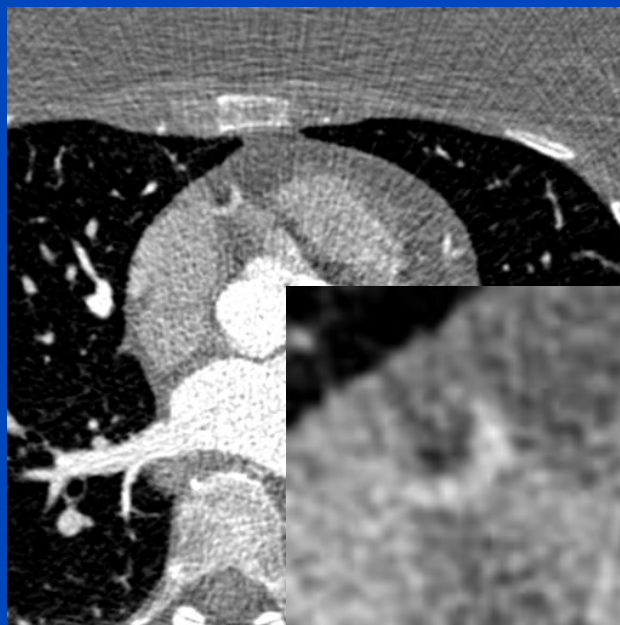
Deep PAMoCo



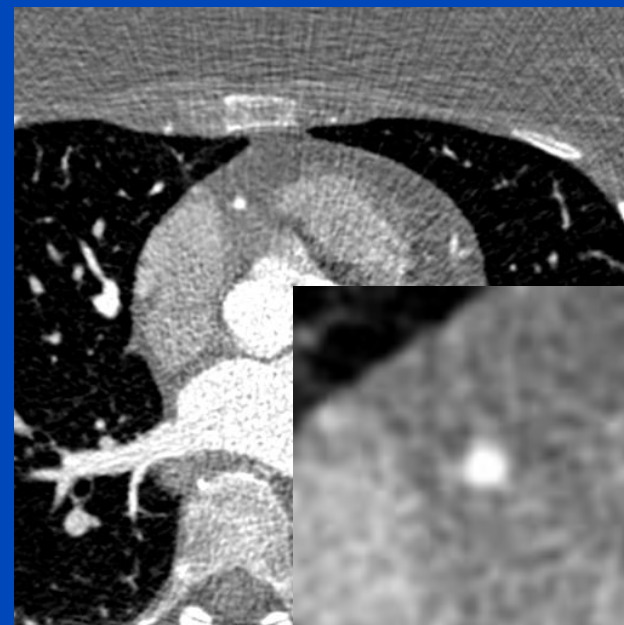
$C = 0 \text{ HU}$, $W = 1400 \text{ HU}$

Patient 2

Original



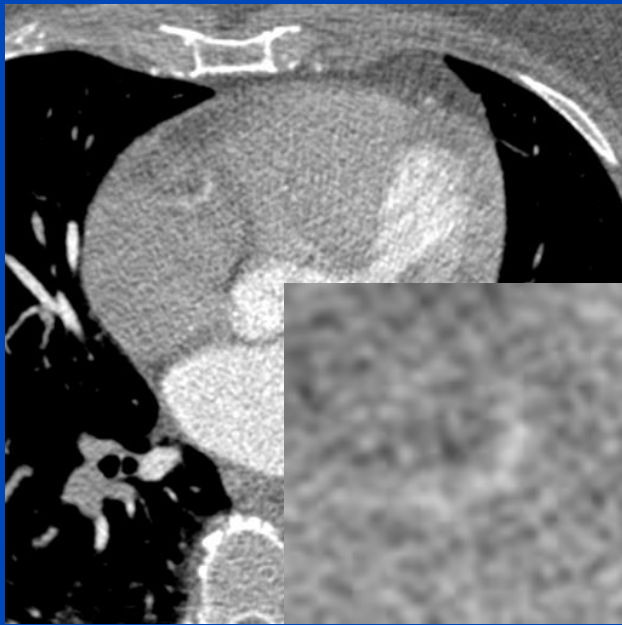
Deep PAMoCo



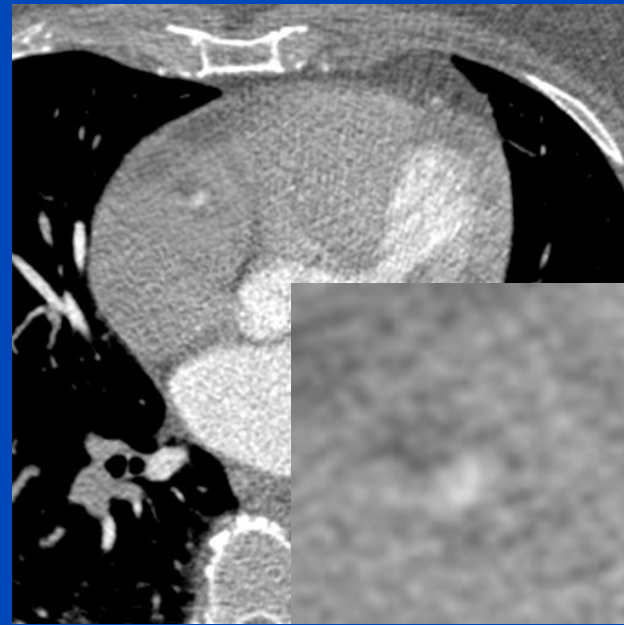
$C = 0 \text{ HU}$, $W = 1600 \text{ HU}$

Patient 3

Original



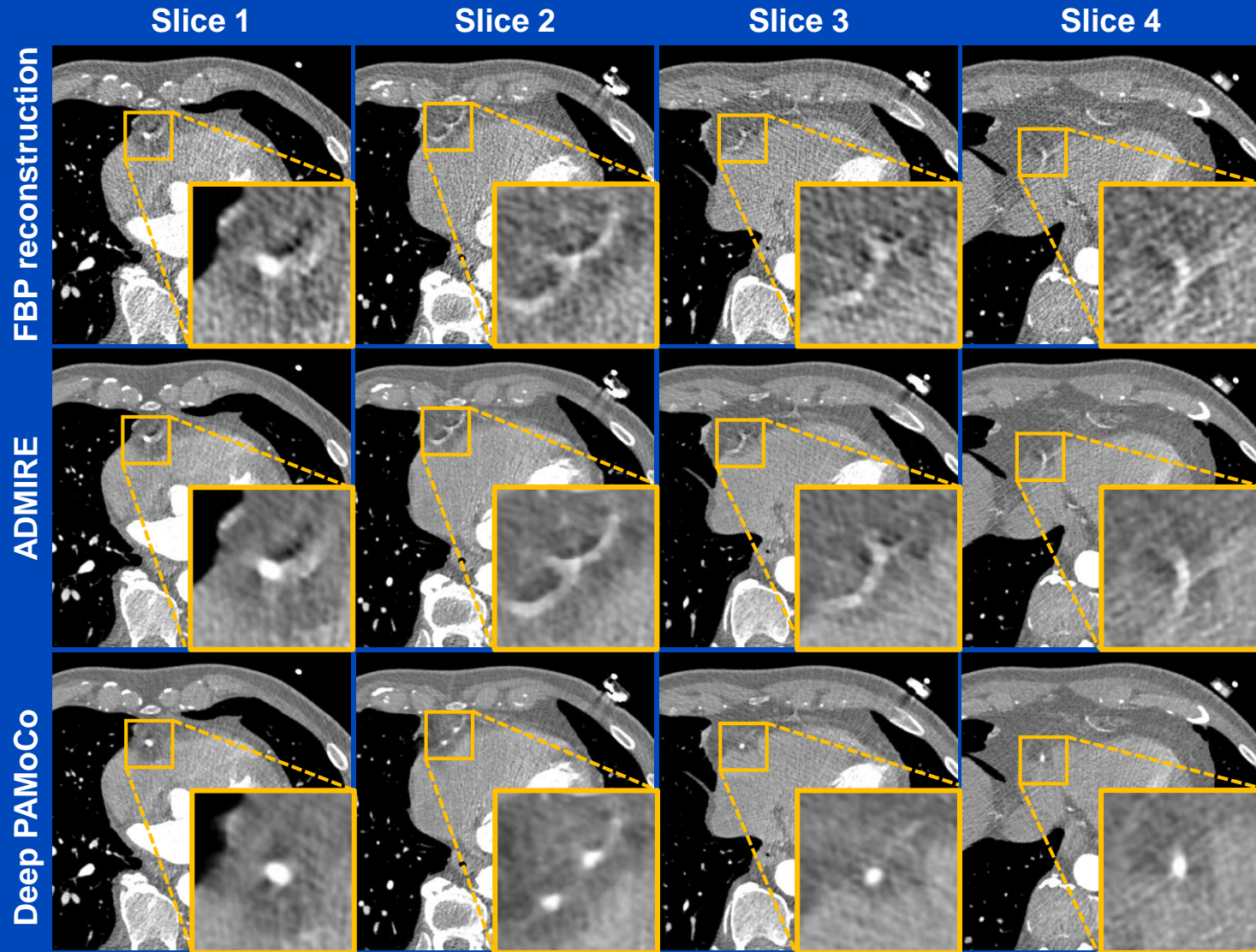
Deep PAMoCo



$C = 0 \text{ HU}$, $W = 1000 \text{ HU}$

Patient 4

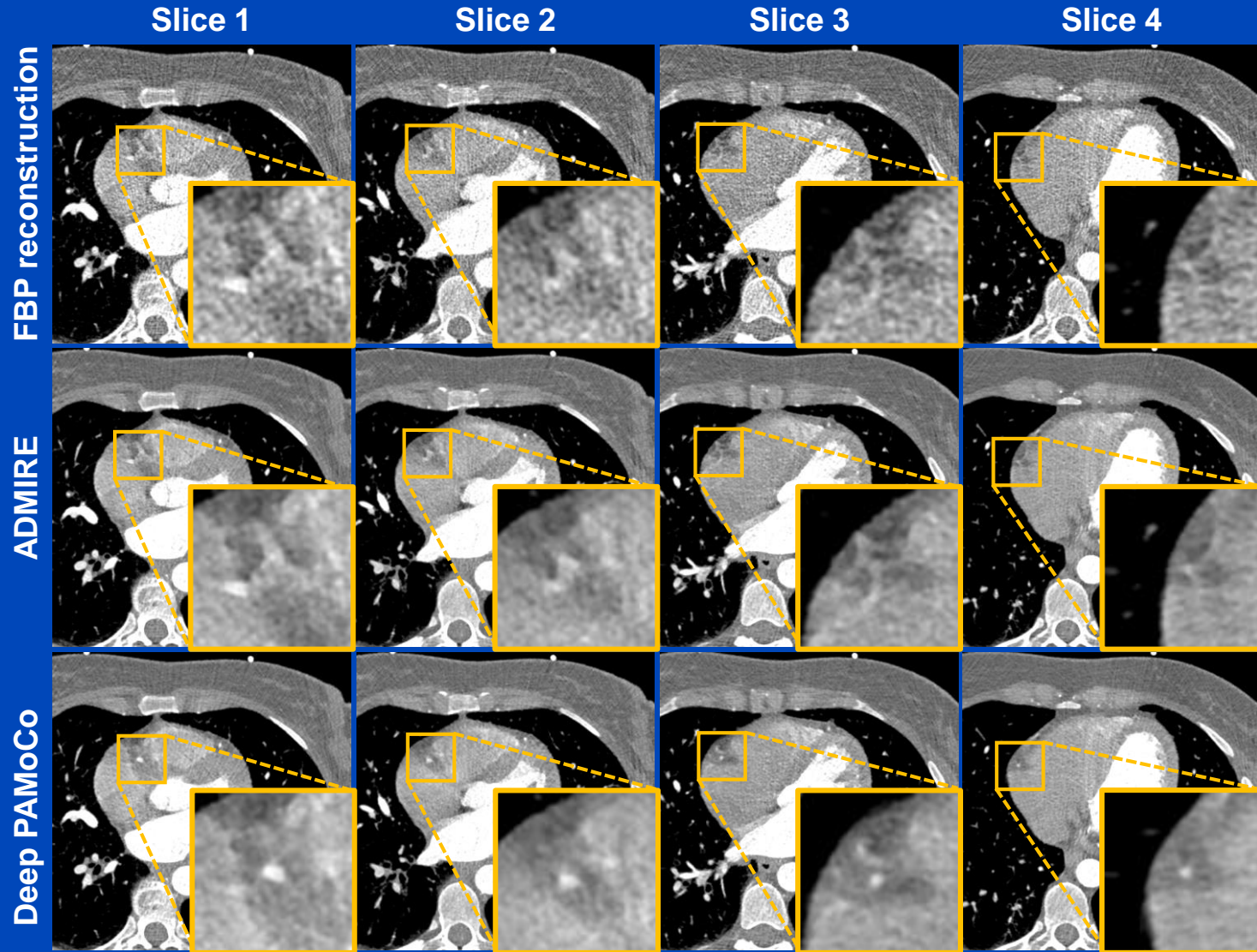
Measurements at a Siemens Somatom AS



$C = 0 \text{ HU}$, $W = 1200 \text{ HU}$

Patient 5

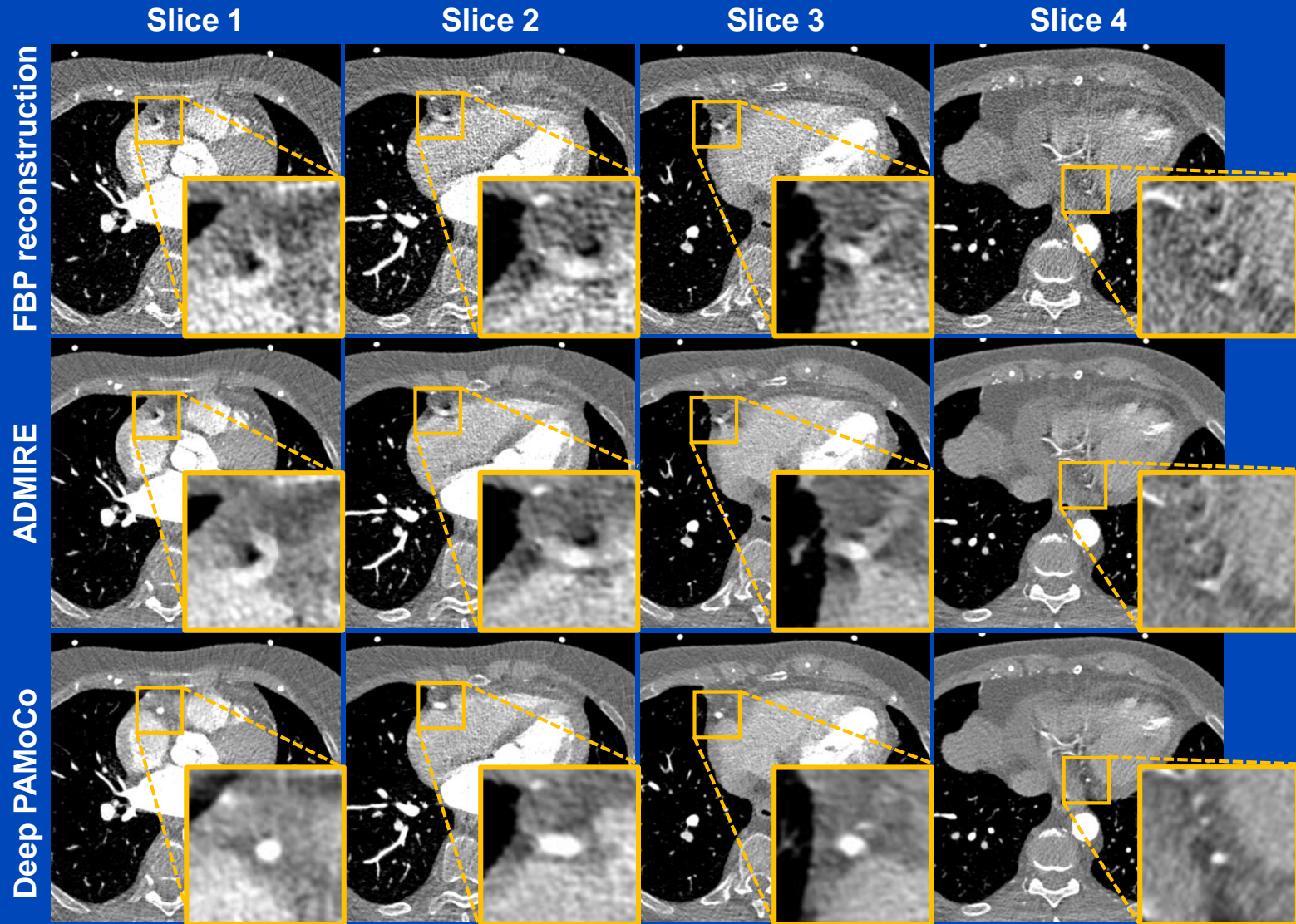
Measurements at a Siemens Somatom AS



$C = 0 \text{ HU}$, $W = 1200 \text{ HU}$

Patient 6

Measurements at a Siemens Somatom AS



$C = 0 \text{ HU}$, $W = 1400 \text{ HU}$

Thank You!

This presentation will soon be available at www.dkfz.de/ct.
Job opportunities through DKFZ's international PhD or
Postdoctoral Fellowship programs (marc.kachelriess@dkfz.de).
Parts of the reconstruction software were provided by
RayConStruct® GmbH, Nürnberg, Germany.